

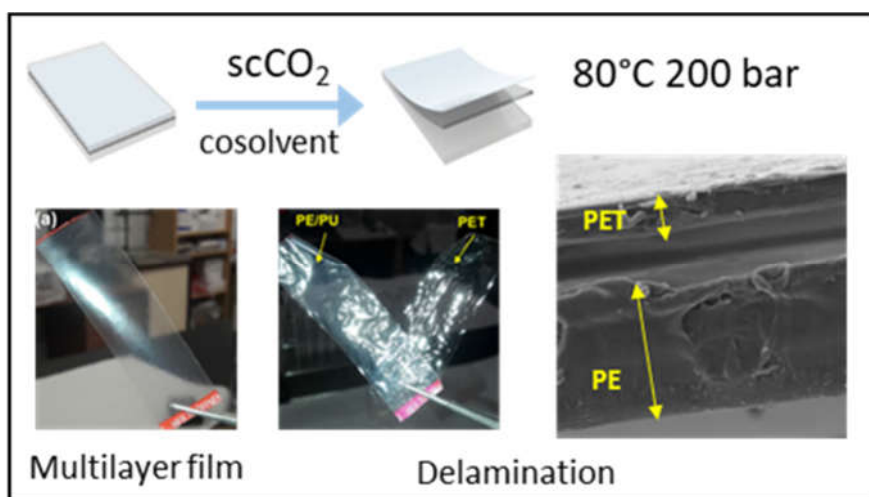
Sustainable Delamination of Multilayer Plastic Films for Advanced Recycling

Ramiro J. Olmos-Greco¹, Eduardo Pérez¹, Lourdes Calvo², Albertina Cabañas^{1, *}

¹Department of Physical Chemistry, ²Department of Chemical and Materials Engineering, Complutense University of Madrid, 28040 Madrid, Spain

*Corresponding author's email: a.cabanas@quim.ucm.es

GRAPHICAL ABSTRACT



Highlights

Sustainable Delamination of Multilayer Plastic Films for Advanced Recycling

**Ramiro J. Olmos-Greco¹, Eduardo Pérez¹, Lourdes Calvo²,
Albertina Cabañas^{1, *}**

- A new sustainable delamination process for multilayer plastic films is proposed
- The method involves supercritical CO₂ treatment and rapid depressurisation
- Small amounts of cosolvents are added to facilitate the process
- Delamination of commercial PE/PET, MDO-PE/PE and PolyAl is achieved.
- A multiple mechanism for the process is proposed

1 **Sustainable Delamination of Multilayer Plastic Films for Advanced**
2 **Recycling**

3 **Ramiro J. Olmos-Greco¹, Eduardo Pérez¹, Lourdes Calvo², Albertina**
4 **Cabañas^{1, *}**

5 ¹*Department of Physical Chemistry, ²Department of Chemical and Materials*
6 *Engineering, Complutense University of Madrid, 28040 Madrid, Spain*

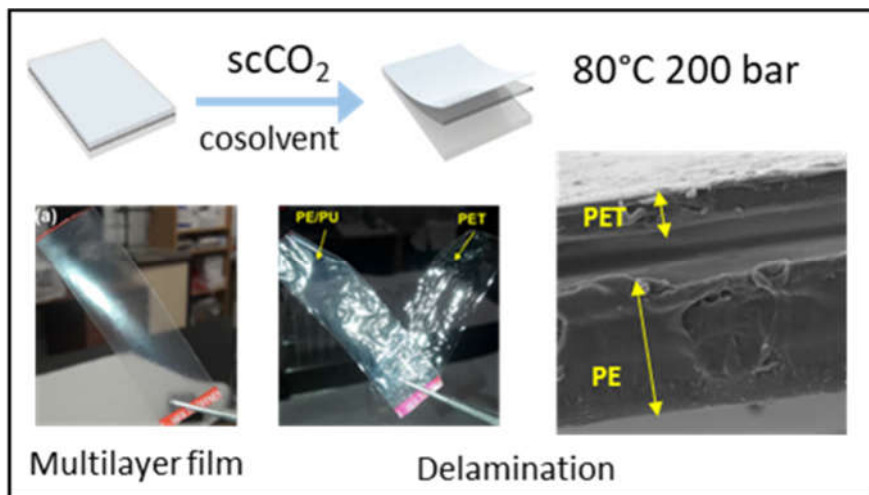
7 *Corresponding author's email: a.cabanas@quim.ucm.es

8

9

GRAPHICAL ABSTRACT

10



11

12

13

14 **ABSTRACT**

15 A novel delamination process for multilayer plastic films using supercritical CO₂
16 is proposed as a sustainable alternative to facilitate their recycling. The method
17 involves exposing the films to pure CO₂ or CO₂ modified with a small amount of
18 cosolvent under mild conditions (40–80 °C, up to 200 bar), followed by rapid
19 depressurisation. As proof of concept, the delamination of three commercial films
20 used in food packaging is presented. The starting material and the delaminated
21 layers were analysed by ATR-FTIR, TGA, DSC and SEM microscopy. Multilayer
22 polymer films formed by polyethylene (PE) and polyethylene terephthalate (PET)
23 or PE and Machine Directed Oriented PE (MDO-PE) prepared with polyurethane
24 adhesive (PU) were delaminated at the PET/PU and MDO-PE/PU interfaces.
25 Furthermore, PolyAl from an aseptic beverage carton delaminated partially,
26 releasing a thin PE layer and an aluminium-enriched PolyAl composite. DMSO
27 and methanol showed the highest delamination efficiency among the cosolvents,
28 while acetone and water were ineffective under the conditions studied. A multiple
29 mechanism for the process is proposed: (1) mechanical stress due to CO₂-
30 induced polymer swelling and rapid depressurisation; (2) selective adhesive
31 debonding via cosolvents. Further studies are needed to corroborate the
32 mechanism, validate the process across varied materials, and optimise its
33 performance. This technology could contribute significantly to a more circular and
34 sustainable economy.

35

36

37 1. INTRODUCTION

38 Synthetic polymers (plastics) are among the most ubiquitous materials in current
39 society. The accumulation of plastic waste, due to pollution and the presence of
40 microplastics, causes serious environmental and public health problems.

41 Furthermore, there has been a worldwide paradigm shift in waste processing in
42 recent decades. This change aims to reincorporate the constituent materials of
43 products that have reached the end of their useful life to ensure a circular
44 economy. For that, innovative, effective and low-cost strategies are needed in
45 each of the steps of plastic recycling [1, 2].

46 In 2022, the European plastic production was 58.7 million tonnes (Mt), where 7.7
47 Mt of plastics were recycled, which represented 16 % of plastic production [3].
48 The EU has demanded that at least 25 % recycled material should be added to
49 plastics production from 2025 onwards. Thus, the European Commission's
50 'Circular Plastics Alliance' aims to incorporate 10 million tonnes of recycled
51 plastics by that date.

52 The food industry generates the largest volume of plastic waste. Plastics are used
53 primarily in food packaging (primary wrapping) as one of the most effective ways
54 to address food safety issues [4]. They also provide protection during transport
55 (secondary and tertiary wrapping).

56 Multilayer films consist of two or more layers of different materials. They are
57 essential for primary food packaging due to their specific properties and
58 advantages, such as barrier properties, mechanical strength, lightweight,
59 flexibility and other functional properties [5]. The combination of different layers
60 improves the barrier properties against gases, water, oil and ultraviolet light,
61 which helps to preserve the freshness, flavour and quality of food while
62 preventing its oxidation. They can also incorporate layers with active functions,
63 such as antimicrobial and antioxidant properties, which contribute to food safety
64 and extended shelf life [6]. A well-known example of multilayer film is the Aseptic
65 Beverage Cartons (ABC), more commonly known as Tetra Brik[®], which consists
66 of several superimposed layers of polyethylene, cardboard and aluminium.

67 Different overlapping polymeric layers form other composites. The most common
68 multilayer films involve low-density or high-density polyethylene (PE),
69 polyethylene terephthalate (PET) and/or polypropylene (PP). A polyurethane
70 (PU) adhesive can be used to bond the layers together.

71 Multilayer plastics, which make up about 20 % of flexible packaging [7], are
72 difficult to recycle due to their diverse polymer compositions and inadequate
73 detection and collection systems. The current recycling techniques used for
74 multilayer packaging have been recently reviewed [7]. The pollution

75 characteristics of typical waste plastic recycling plants have also been analysed
76 [8]. Physical recycling of multilayer materials can be performed by the selective
77 dissolution/precipitation technique. In this method, each polymer is dissolved or
78 melted selectively, to be later precipitated and reused. Although effective, this
79 method requires using toxic organic solvents that are dangerous to the
80 environment and/or high temperatures, so it is not considered sustainable.
81 Furthermore, organic solvent residues may be left in the recycled polymer,
82 restricting its use. The process can be coupled with chemical recycling of the
83 recovered layers to get the corresponding monomers.

84 Selective degradation of some of the layers (chemical etching) can also be
85 carried out. For example, PET combined with PE can be selectively
86 depolymerised to recover terephthalic acid in concentrated H₂SO₄ [9]. However,
87 this process generates a large amount of aqueous liquid waste that needs to be
88 further treated before disposal.

89 Delamination of multilayer films has also been attempted. Dissolution of the
90 adhesive between layers has been described using nitric acid or bases [10].
91 However, the process is highly polluting and can also partially degrade the layers.
92 Although mechanical delamination of multilayer films is rarely attempted due to
93 the strong binding between the individual layers in the multilayer film, the
94 delamination of multilayer PE/PU/PET films subjected to hydrostatic pressure has
95 been previously reported [11]. The authors attributed this phenomenon to
96 interfacial stress associated with the different mechanical properties of the films,
97 PET being the hardest. After delamination, separation based on different layer
98 densities, electrostatic charge or melt can be performed.

99 During the ABC recycling process, the cardboard and outer PE films are easily
100 separated, dispersing the cellulose fibres by hydropulping. The remaining
101 material is a composite of polyethylene and aluminium layers commonly known
102 as PolyAl, which contains around 15 % aluminium. PolyAl can be recycled
103 mechanically to produce a wide variety of composite materials used in
104 construction by a combination of techniques such as agglutination, extrusion,
105 moulding, etc. Other possible recycling techniques, such as pyrolysis, selective
106 dissolution and solvent delamination, typically require high temperatures or
107 harmful solvents [12].

108 The application of supercritical fluids to plastic recycling is an expanding area
109 [13]. Supercritical fluids have a solvation power like liquids, but their transport
110 properties (diffusivity, viscosity) are more similar to those of gases. Supercritical
111 CO₂ (scCO₂) stands out because it is cheap, non-combustible, innocuous, has
112 moderate critical parameters (31.0 °C and 73.8 bar), is a gas at ambient
113 temperature and does not leave any residue. CO₂ solubilises very well in the
114 amorphous regions of polymers, swelling them and causing a decrease in their
115 glass transition temperature (T_g). Rapid depressurisation of the swollen polymer

116 can lead to foaming. CO₂ also decreases the melting temperature of polymers
117 [14]. These properties can be used favourably in physical recycling processes. In
118 addition, CO₂ can improve mass transfer between polymer chains by increasing
119 reactivity, which also favours chemical recycling processes. Thanks to their high
120 diffusivity, supercritical fluids can penetrate solid matrices easily, making them
121 excellent extraction agents and, therefore, useful for the removal of impurities in
122 polymers [15] and in polymer decontamination [16]. Finally, sterilisation of
123 biological plastic residues for reuse and/or recycling is also possible [17].

124 In this paper, we propose using scCO₂ alone or modified with cosolvents to
125 delaminate multilayer packaging films. The starting hypothesis is that the different
126 polymer films in a multilayer system swell differently in contact with CO₂,
127 generating mechanical stresses between the films and, therefore, inducing
128 separation/delamination of the layers. The addition of a cosolvent can help in the
129 process, and partial dissolution or degradation of the polymer at the interface
130 could take place.

131 There is enough evidence in the literature to support both effects. The
132 Supercritical Carbon Dioxide Resist Removal (SCORR) process, developed at
133 Los Alamos Laboratory in 1998 to clean semiconductor remnants from the
134 lithographic process, was based on using liquid or scCO₂ to solubilise into the
135 polymer residues [18]. Swelling of the residual polymeric photoresist, followed by
136 a sudden depressurisation, led to the separation of the polymer from the
137 substrate. A cosolvent could also be added to CO₂ to facilitate separation. The
138 application of CO₂ pressure pulses facilitated the process [19].

139 More recently, Aymonier and Slostowski [20] patented a method to delaminate
140 multilayer systems, including at least one organic layer, using scCO₂ modified
141 with non-reactive solvents. They provided different examples of delamination of
142 interest in the photovoltaic industry and proposed that the method could be
143 applied to the food, pharmaceutical and cosmetic industries. Delamination was
144 always performed between a polymeric material in contact with a non-polymeric
145 one (glass, metal, or cardboard). This approach has been further studied by
146 Briand *et al.* in the recycling of photovoltaic panels [21-23]. Swelling of the
147 encapsulated polymer following rapid depressurisation led to polymer foaming
148 and mechanical stress and promoted loss of adhesion at the interface.
149 Delamination was also observed by Sumey *et al.* in the foaming of polystyrene
150 and poly(methyl methacrylate) multilayer thin films [24]. Separation of metal–
151 polymer composites using CO₂-induced bubble nucleation has been recently
152 proposed for aluminium–polycarbonate composites [25]. Furthermore, CO₂
153 exfoliation processes based on the binder dissolution have been employed in the
154 recycling of lithium-ion batteries [26, 27].

155 Despite extensive research indicating scCO₂ efficacy for delamination, a
156 significant knowledge gap exists regarding its application to multilayer polymer

157 composites used in packaging. This study aims to address this gap by presenting
158 exploratory research, demonstrating for the first time the feasibility of scCO₂
159 delamination on three commercial multilayer composites: two polymer films and
160 a PolyAl composite. A plausible mechanism for the delamination process in CO₂
161 is proposed.

162 **2. MATERIALS AND METHODS**

163 **2.1. Chemicals and polymer films**

164 Carbon dioxide (CO₂) (99.995 % pure) was provided by Air Liquide. Ethanol
165 (Scharlau, ≥ 99.9 %), methanol (Fisher Chemical, ≥ 99.8 %), dimethyl sulfoxide
166 (DMSO) (Fisher Chemical, ≥ 99.9 %), acetone (Honeywell, ≥99.8 %) and
167 deionised water were used as cosolvents. All reagents were obtained from
168 Spanish providers and employed as received without further purification.

169 The multilayer polymer films used for food packaging were kindly donated by
170 Plastigaur S.A. (Gipuzkoa, Spain). Samples were formed by a stack of PE and
171 PET or PE and Machine Directed Oriented PE (MDO-PE) using polyurethane
172 (PU) as adhesive.

173 Low-density PE films are flexible, soft, transparent, shiny, and highly resistant to
174 moisture, tearing, and chemicals. PET films are more rigid and provide good
175 barrier properties. MDO-PE (harder than conventional PE) is proposed as a
176 replacement for PET in multilayer films to ease recycling.

177 For the two commercial multilayer polymer films, the thickness of the PET layer
178 was 12 μm. PE and MDO-PE layers were 50 μm and 25 μm, respectively. Films
179 had a 2 μm thick PU-based PL272A+CF-60 adhesive from Morchem S.A.
180 (Guadalajara, Spain). The two multilayer composites are designated according to
181 their structure as PE/PU/PET and MDO-PE/PU/PE. Each of the PE commercial
182 layers is, in fact, a multilayer blown film made of 3 or 5 sub-layers of different
183 densities (see **Figure S1**, Supplementary Material).

184 Additionally, simpler PE/PU and PET/PU stacks were prepared by applying a thin
185 layer of a PU adhesive on PE and PET films. For the application of the adhesive,
186 we follow the provider's instructions (see Supplementary Material, Section 2).
187 Before the application of PU adhesive, PE films were subjected to a corona
188 treatment, which is a surface modification technique that uses a low-temperature
189 plasma discharge to improve adhesion by increasing the polarity and roughness
190 of the films. Samples were cut into small pieces with sizes from *ca.* 3 x 1 cm² to
191 1 x 1 cm² for analysis.

192 PolyAl films were obtained from a commercial orange juice Tetra Brik® carton.
193 The material was cut into pieces and treated in distilled water at 60-70 °C for 2 h
194 under stirring, simulating the hydro pulping process. The PolyAl fragments were
195 separated from the cardboard, washed and dried in an oven overnight.

196

197 **2.2. Supercritical fluid delamination process.**

198 Experiments were performed in a ca. 60 mL custom-made high-pressure reactor
199 previously described [28]. The high-pressure set-up includes inlet and outlet high-
200 pressure valves (SS-OV-S2), a pressure gauge and a safety relief valve (SS-
201 4R3A) to prevent overpressure (all Swagelok components). The reactor was
202 housed in an aluminium block heated by heating cartridges controlled using a
203 PID controller and mounted on a stirring plate. The temperature within the reactor
204 was measured using a type J thermocouple placed into the reactor.

205 Several pieces of different plastic films (250-500 mg) were introduced into the
206 reactor. In the experiments using cosolvents, 5 mL of an organic solvent
207 (methanol, ethanol, acetone and DMSO) or water was also placed into the reactor
208 in a small vial with a magnetic stirrer, so it is kept separated from the films. The
209 reactor was closed, and the heater was set at the desired temperature. After the
210 temperature was reached, CO₂ was introduced into the reactor from a Teledyne
211 ISCO syringe pump thermostated at the temperature of the experiments, up to
212 the desired pressure. When cosolvents were used, the reactor was stirred to
213 speed up the mixing of CO₂ and the cosolvents. The system was kept at these
214 conditions for 2 h and depressurised rapidly, opening manually the outlet high-
215 pressure valve. Experiments were performed at 40 °C and 80 °C, and 200 bar.
216 Depending on the temperature, the depressurisation time varied from 20 to 30 s.
217 Assuming a linear depressurisation profile, depressurisation rates between 10-7
218 bar/s were employed. Cosolvent proportions in the supercritical CO₂ phase as
219 well as bibliographic sorption values of CO₂ in the polymers are reported as mass
220 percentages (%)

221 After cooling, the reactor was opened, and the samples were removed from the
222 reactor for further analysis. The samples were dry, except for the experiments
223 performed using DMSO and water, where the samples appeared wetted by the
224 solvent. This is related to the lower miscibility of these solvents with CO₂, due to
225 their much lower vapour pressures and higher boiling points in comparison to the
226 other organic solvents used as cosolvent. Samples wetted by DMSO were further
227 washed with distilled water. Experiments were performed in triplicate.

228 To identify possible substances eluted with the CO₂ upon depressurisation, the
229 experiments with DMSO were repeated using the deuterated solvent and
230 depressurising the reactor through a small vial containing deuterated DMSO. For
231 collection purposes, the depressurisation rate was kept low at ca. 2 bar/min.
232 Sample was analysed by ¹H NMR (Bruker AV 250MHz BACS60).

233 **2.3 Characterisation techniques**

234 Multilayer films were characterised before and after the CO₂ treatment using
235 Attenuated Total Reflectance Fourier Transform Infrared Spectroscopy (ATR-

236 FTIR), Differential Scanning Calorimetry (DSC), Thermogravimetric Analysis
237 (TGA) and Scanning Electron Microscopy (SEM).

238 ATR-FTIR spectra were collected using a Perkin Elmer Spectrum 100 apparatus
239 at a spectral resolution of 4 cm⁻¹ between 4000 and 650 cm⁻¹ and 16
240 accumulations.

241 DSC of the films was performed using a Q20 TA Instrument. Measurements were
242 performed in dry N₂, flowing at 10 mL/min. The temperature and enthalpy of the
243 calorimeter were previously calibrated using standard samples of Indium (99.999
244 %). Films were heated from -40 to 270 °C at a heating rate of 10 °C/min. Glass
245 transition temperatures, melting temperatures and heats of fusion were
246 determined from the first heating cycle using the Universal TA Analysis software.

247 TGA analysis of the films was performed using an SDT- Q600 from TA from 35 to
248 600 °C at a heating rate of 10 °C/min under 100 mL/min N₂ flow.

249 SEM was performed using two JEOL microscopes: JSM IT700HR and JSM-7600.
250 Cross-sections for analysis were prepared by cooling the samples with liquid N₂
251 before fracturing with a pair of scissors. Samples were analysed before and after
252 the supercritical treatment. Additionally, the internal face of some delaminated
253 samples was studied under the microscope. Samples were gold-coated. Images
254 from both secondary and backscattered electrons were recorded. Energy
255 Dispersive X-ray (EDX) analysis was also performed in different regions of the
256 films for identification purposes.

257

258 **3. RESULTS AND DISCUSSION**

259 First, the delamination behaviour of custom-made bilayer systems formed by PET
260 or PE and a PU adhesive layer was evaluated, focusing on the influence of
261 temperature and density during the scCO₂ treatment. The success of these
262 experiments led us to attempt the delamination of more complex commercial
263 multilayer films. In this case, different cosolvents were introduced to identify the
264 most effective one, based on delamination performance, toxicity, and recyclability.
265 The composition of the resulting layers and the interface where delamination
266 occurred were analysed using FTIR, DSC and SEM techniques.

267 **3.1. Delamination of lab-prepared bilayer polymer films**

268 The first experiments were performed on the PE/PU and PET/PU lab-prepared
269 films. PE and PET polymers are the most common materials used in packaging.
270 Experiments were performed at 40 and 80 °C at 200 bar using pure CO₂, followed
271 by sudden depressurisation.

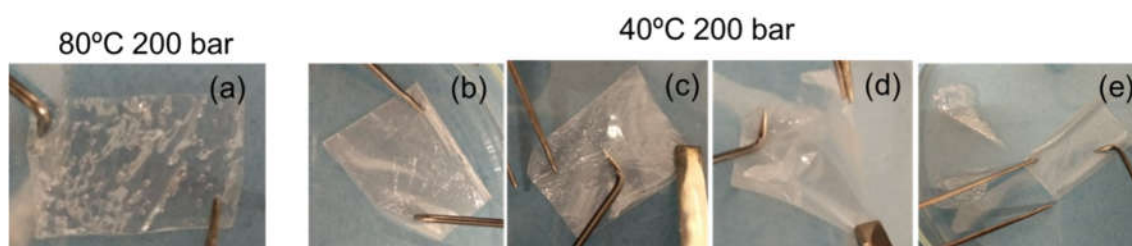
272 Visual inspection of the PET/PU samples after the CO₂ treatment, followed by
273 rapid depressurisation, showed bubble formation and partial delamination of the

274 films (**Figure 1a**). In contrast, PE/PU films did not show appreciable changes after
275 the CO₂ treatment at the same conditions.

276 Using a pair of tweezers, PET and PU layers could be easily separated (**Figure**
277 **1b-e**). Additionally, films curved when exposed to CO₂, indicating a different
278 interaction of CO₂ with the different layers. The convex side of the curved films
279 corresponded to the PU adhesive. The best results were obtained at 40 °C and
280 200 bar, conditions of higher CO₂ density. Rapid depressurisation was essential
281 to promote delamination. Thus, it was clear that CO₂ has a physical effect on the
282 polymer films.

283 This was somehow surprising as the interaction of PET with the PU adhesive is
284 expected to be stronger than the interaction of PE and PU. PET and PU can
285 interact through covalent or hydrogen bonding, whilst the interaction of PE and
286 PU, even after the introduction of some functional groups following the corona
287 treatment, may be weaker. In fact, blends of PU and PET have been prepared,
288 indicating good polymer compatibility and strong interface adhesion [29]. In
289 contrast, the low surface energy and wettability of PE require corona and
290 chemical treatments to improve the PU adhesion [30].

291 To understand the different behaviour of PET/PU and PE/PU interfaces when
292 exposed to CO₂, the effect of CO₂ on the different polymers should be considered.
293 It is well known that CO₂ dissolves appreciably in the amorphous domains of
294 semicrystalline polymers, causing polymer plasticisation and swelling [14]. The
295 effect depends on the chemical composition of the polymer and its interaction
296 with CO₂, as well as on the crystallinity and mechanical properties of the polymers
297 that may restrict polymer dilation.



298
299 **Figure 1.** Photographs of PET/PU films treated with supercritical CO₂: (a) 80 °C
300 and 200 bar, (b–e) 40 °C and 200 bar. The images show partial delamination at
301 the adhesive interface, evidenced by the manual separation of the layers using
302 tweezers.

303 The sorption of CO₂ in PET at 40 °C and 150 bar is ca. 8 %, although the swelling
304 is almost negligible at these conditions due to the high rigidity and crystallinity of
305 PET [31]. At 80 °C and 200 bar, the CO₂ sorption is lower than 3 %, but a small
306 swelling between 2 and 3 % is reported [32]. Comparatively, the sorption of CO₂
307 in low-density PE films is smaller than that in PET at the same conditions [33].

308 However, the swelling is slightly larger. For example, at 60 °C and 200 bar, a 4-
309 5% swelling of PE has been reported [34].

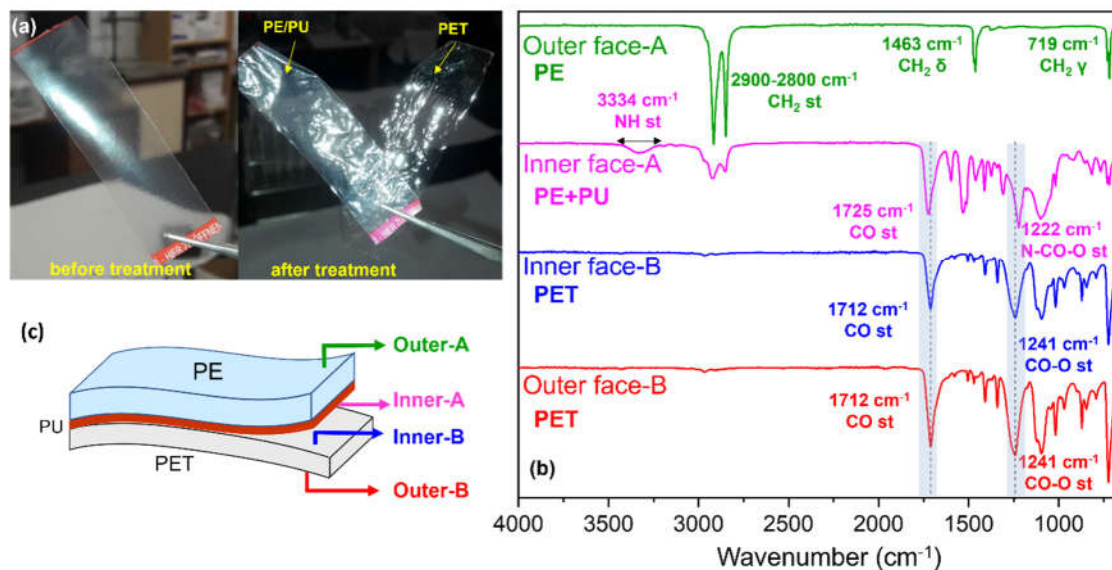
310 In contrast, for the PU adhesive with different molecular weights and cross-linking
311 densities, values for CO₂ sorption and swelling at 80 °C and 150 bar are between
312 7-30% and 20-30%, respectively [35]. Thus, the PU adhesive, although highly
313 cross-linked, may sorb a larger CO₂ quantity and swell appreciably, in comparison
314 to PE and PET, promoting the film delamination in PET/PU, where the mismatch
315 in swelling and mechanical properties is larger.

316 **3.2. Delamination of commercial multilayer polymer films**

317 Experiments were conducted using the commercial multilayer polymer films
318 PE/PU/PET and MDO-PE/PU/PE. Experiments were performed at 40 and 80 °C
319 and 200 bar. In both samples, exposure to pure CO₂ failed to induce
320 delamination, although some bubble formation was observed in the films. Best
321 results were obtained at 80 °C. In contrast to the PET/PU samples prepared in
322 the lab, commercial samples had a much thinner PU layer sandwiched between
323 the other polymer layers.

324 Further experiments were performed at 80 °C and 200 bar, adding 5 mL of
325 methanol as cosolvent, which corresponded to 11 %. At these conditions, CO₂
326 and methanol were fully miscible [36, 37]. PE/PU/PET films followed by rapid
327 depressurisation were successfully delaminated into two layers and separated
328 easily using a pair of tweezers, as shown in **Figure 2a**. The FTIR analysis of the
329 different layers is presented in **Figure 2b**. Layer B was identified as PET, showing
330 the characteristic strong bands at 1712 cm⁻¹ associated with the carbonyl
331 stretching and 1250 cm⁻¹ to the ester group, in both the outer and inner faces of
332 the layer. FTIR of the outer layer A showed two sharp and intense absorption
333 bands at 2800 – 2900 cm⁻¹ ascribed to the CH₂ asymmetric and symmetric
334 stretching bands and medium and sharp bands at 1463 and 719 cm⁻¹
335 corresponding to the bending and rocking of PE. The inner face of layer A showed
336 the PE characteristic bands superimposed to bands associated with PU,
337 particularly the band at 1222 cm⁻¹ due to C-N stretching, the band at 1725 cm⁻¹
338 due to carbonyl stretching (urethane moiety) and a broad band at 3334 cm⁻¹ due
339 to N-H stretching. FTIR-ATR beam penetration was enough to detect both the PU
340 thin layer and the PE outer layer. Thus, as shown in **Figure 2c**, delamination took
341 place at the PET/PU interface.

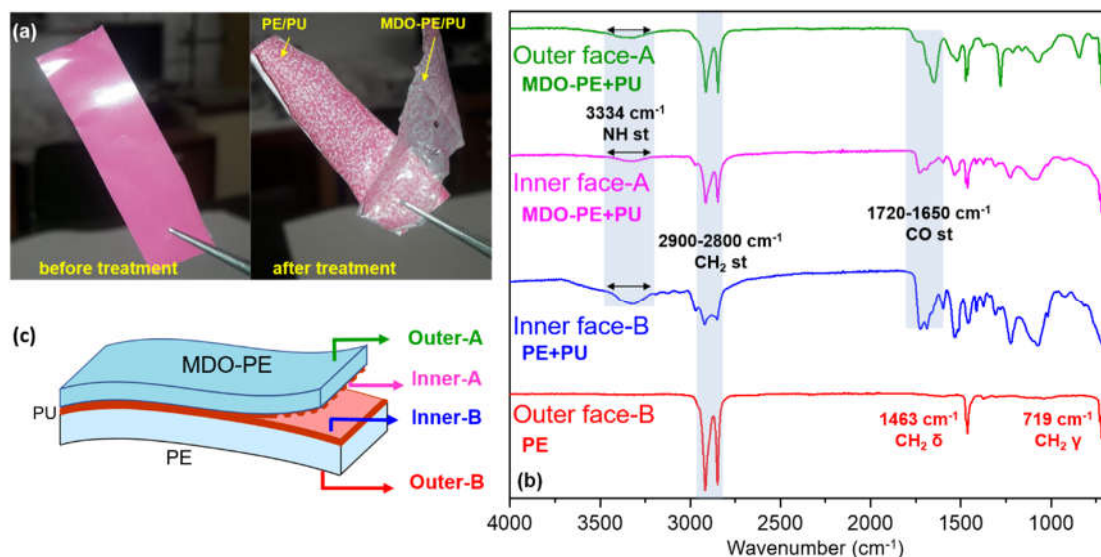
342 Similarly, MDO-PE/PU/PE films treated at 80 °C and 200 bar followed by rapid
343 depressurisation, were also easily separated using a pair of tweezers (**Figure**
344 **3a**). In this case, the commercial sample was coloured. The PE layer appeared
345 white due to the presence of TiO₂ particles, while the MDO-PE side exhibited a
346 magenta colour, resulting from the application of magenta ink printed on the inner
347 surface of the PE film.



349

350 **Figure 2.** (a) Photographs of PE/PU/PET films before and after treatment with
 351 CO₂ modified with 11 wt% methanol as cosolvent, at 80 °C and 200 bar. (b) ATR-
 352 FTIR analysis of the different layers and their identification. (c) Schematic of the
 353 delamination process according to FTIR.

354



355

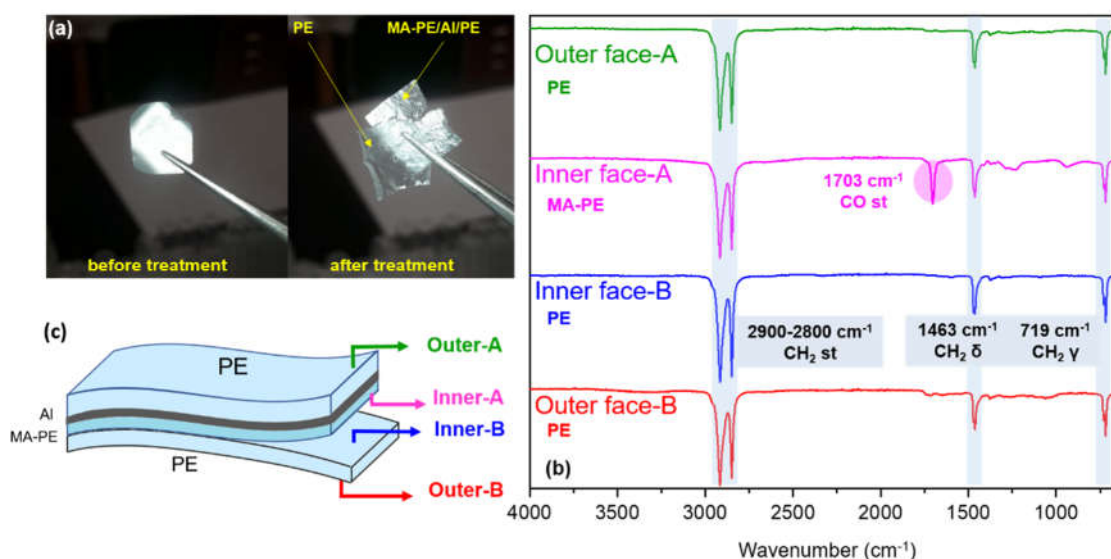
356 **Figure 3.** (a) Photographs of the MDO-PE/PU/PE film before and after the
 357 treatment with CO₂ modified with 11 wt% methanol as cosolvent at 80 °C and 200
 358 bar. (b) ATR-FTIR analysis of the different layers and their identification, and (c)
 359 schematic of the delamination process according to FTIR.

360 After delamination, A and B layers were analysed by FTIR (**Figure 3b**). Both
361 layers exhibited the characteristic bands of PE. Outer layer B only showed these
362 bands, but outer layer A presented additional bands that were associated to the
363 pigments and additives of the magenta ink. FTIR analysis of the inner part of
364 layers A and B showed bands due to the PU adhesive or other additives
365 superimposed to those of PE. Pictures of the layers after delamination showed
366 that, in this multilayer film, separation was not clean, resulting in partial material
367 transfer between layers. Adhesive and pigment residues remained on both
368 delaminated surfaces, as shown in **Figure 3c**. The broad band below 750 cm^{-1}
369 visible in both inner faces was ascribed to TiO_2 present in the PE layer [38].
370 Differences in the levels of CO_2 sorption within the MDO-PE and PE layers are
371 expected due to their different crystallinity.

372 Experiments were also performed using PolyAl multilayer films. Although PolyAl
373 is formed by a complex multilayer structure, after the CO_2 treatment, two different
374 layers could be separated using tweezers (**Figure 4a**). FTIR analysis of A and B
375 layers (**Figure 4b**) showed bands due to PE in both the inner and outer faces. At
376 the inner face of layer A, a relatively strong band at 1701 cm^{-1} , along with weak
377 bands at $1200\text{-}1300\text{ cm}^{-1}$, and 940 cm^{-1} associated with carboxylic acid groups,
378 were identified. These peaks appear in PE films doped with maleic anhydride or
379 in ethylene methacrylic acid copolymers that are used to improve adhesion with
380 the Al layer (MA-PE).

381 Assuming the PolyAl is a composite of four layers whose structure is PE/Al/MA-
382 PE/PE (from outer to inner), the delamination took place at the MA-PE/PE
383 interface to yield a layer of PE and a PE/Al/MA-PE composite that can be
384 envisaged as a PolyAl with a higher proportion of aluminium. The much higher
385 CO_2 sorption and swelling of acrylic polymers[39] in comparison to PE would
386 partially explain why delamination took place at the MA-PE/PE interface [33, 34].

387



388

389 **Figure 4.** (a) Photographs of PolyAl film before and after the treatment with CO₂
 390 modified with 11 wt% methanol as cosolvent at 80 °C and 200 bar, (b) ATR-FTIR
 391 analysis of the different layers and their identification. (c) Schematic of the
 392 delamination process according to FTIR.

393 Samples of the individual PE and PET plastic sheets used for the lamination of
 394 PE/PU/PET were also obtained from the supplier. The area density of the sheets
 395 was determined by weighing pieces of known area of each sheet. The area
 396 densities for PE, PET and PE/PU/PET were 4.53, 1.69 and 6.37 mg/cm²,
 397 respectively. Assuming that the thickness of the sheets did not significantly
 398 change upon lamination, an estimated area density for the PU adhesive layer of
 399 0.16 mg/cm² was calculated. Using the layer thicknesses reported previously,
 400 volumetric densities of 0.91 and 1.41 g/cm³ for PE and PET were obtained. These
 401 densities agree well with values from the literature (Low density PE: 0.91-0.93
 402 g/cm³, PET: 1.33-1.45 g/cm³) [40]. Thus, the density of PU adhesive was
 403 estimated as 0.8 g/cm³. The lower density of PU indicates a larger free volume
 404 that may lead to higher CO₂ sorption and swelling.

405 For the PolyAl, the proportion in mass of the different layers obtained after
 406 delamination using CO₂ modified with methanol was 59 % PE/Al/MA-PE and 41
 407 % PE. Then, the PE/Al/MA-PE layer would contain 25 % of aluminium. This
 408 enriched PolyAl opens new possibilities to use this material in construction [12].

409 The successful delamination of the multilayer films and the composition of the
 410 films analysed by FTIR was further confirmed by thermal analysis. DSC was
 411 performed on the multilayer commercial films, some of the single component
 412 films, PU adhesive and the delaminated A and B layers of each multilayer film
 413 (**Figures 5-7**).

414 **Table 1** summarises the thermal transitions found in each case. It shows the
 415 melting temperatures (T_m), and heats of fusion (ΔH_m) in the films and different
 416 polymer layers. The results confirm the layer identification performed by FTIR.
 417 The transition temperatures of the delaminated layers matched those detected in
 418 the composite and the starting layers. Molar enthalpies were lower for the
 419 composites because of the lower proportion of the crystalline material.

420 **Table 1.** Thermal transitions observed in the multilayer materials, PET and PE
 421 films and the different layers after the CO₂ + methanol treatment.

Film	Layer A		Layer B		Exothermic peak
	T_m (°C)	ΔH_m (J/g)	T_m (°C)	ΔH_m (J/g)	T (°C)
PE/PU/PET	111	79	256	10	174
PE	113	118	-	-	191
Layer A (PE + PU)	113	113	-	-	196
Layer B (PET)	-	-	258	47	170
PET	-	-	257	47	188
MDO-PE/PU/PE	126/135	105	126	105	176
MDO-PE	127/133	150	-	-	-
Layer A (MDO-PE + PU)	126/132	151	-	-	174
Layer B (PE + PU)	-	-	126	123	-
PolyAI (PE/MA-PE/AI/PE)	-	-	108	80	190
Layer A (MA-PE/AI/PE)	97	22	-	-	-
Layer B (PE)	-	-	107	101	190

422

423 **Figure 5** presents the DSC of a PET film, showing the expected T_m for this
 424 polymer at 258 °C [40]. Additionally, two very weak T_g associated possibly to
 425 additives were observed at 52 and 128 °C. The same transitions were identified
 426 in layer B (PET) after delamination. Similarly, the DSC of a PE film showed a very
 427 wide melting transition that started almost at room temperature and had a peak
 428 at 112 °C. This broad transition corresponded to the melting point of a mixture of
 429 different high and medium-density PE layers (**Figure S1**, Supplementary
 430 Material). DSC of layer A (PE + PU) showed the same transitions. The PE
 431 /PU/PET film showed the transitions of both PE and PET. These results support
 432 the successful delamination of the layer according to **Figure 2**.

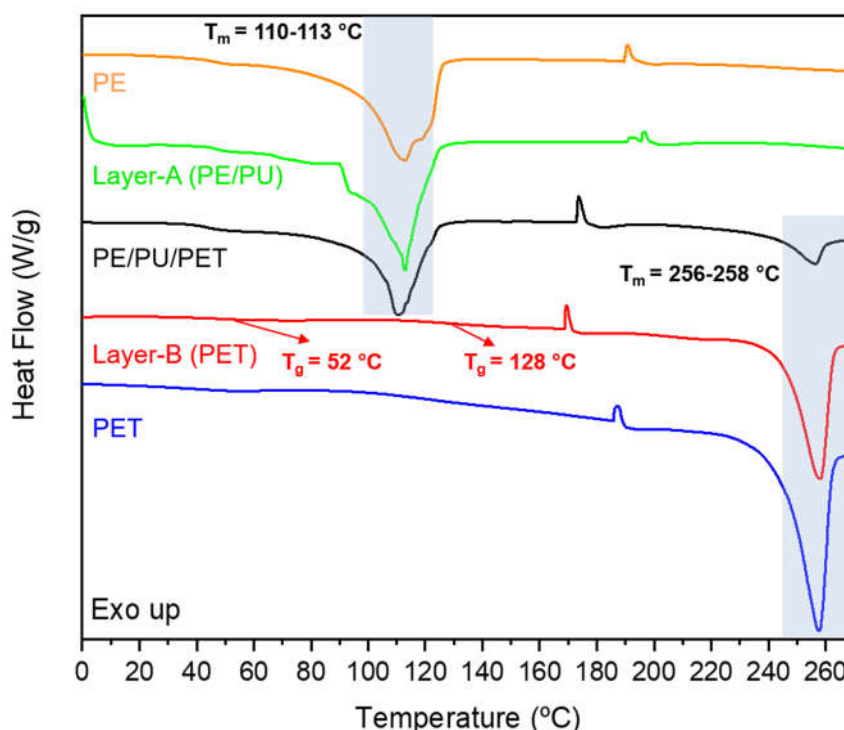
433 An additional narrow and small exothermic peak was found in all the commercial
 434 films studied at a temperature between 170-195 °C. However, TGA analysis of
 435 the PE/PU/PET film (**Figure S2**, Supplementary Material) did not show a clear
 436 mass loss in this temperature range. This peak seems to indicate the presence
 437 of very low quantities of polymer additives or other compounds used to aid
 438 processing in the commercial films.

439 A piece of PU adhesive prepared by mixing the different adhesive components
 440 according to the vendor's instructions (**Section 3**, Supplementary Material), was

441 also studied by DSC. A T_g at ca. 5 °C was observed in the sample, followed by
442 other minor and unclear thermal events (**Figure S3**, Supplementary Material).
443 However, this T_g transition was not observed in layer A (PE + PU), most likely due
444 to the exceedingly small proportion of PU in the layer.

445 Although it has been previously reported that the solubilisation of CO₂ into the
446 amorphous regions of polymers can cause polymer crystallisation [41], the heats
447 of fusion in A and B layers after CO₂ delamination were very similar to those of
448 the single-component films, indicating no changes in the crystallinity of the
449 samples.

450



451

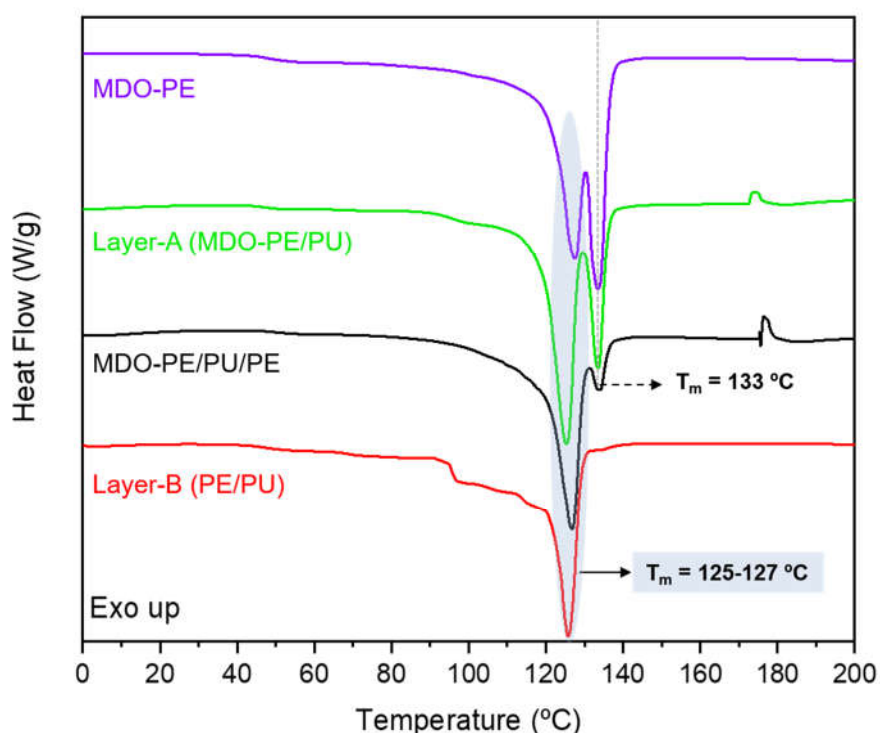
452 **Figure 5.** DSC thermograms of PE/PU/PET, PET and PE films and the layers
453 obtained after the CO₂ + methanol treatment, indicating the different T_g and T_m
454 transitions.

455 Multilayer films were weighed before and after the CO₂ treatment, showing, within
456 the experimental error, that there is no substantial mass loss during the
457 delamination process. Furthermore, TGA analysis of the PE/PU/PET multilayer
458 films, the separated layers A and B (Table 1), and the PU adhesive was also
459 performed (**Figure S2**, Supplementary Material). Layer A (PE + PU) and layer B
460 (PET) decomposed mostly between 420-500 °C and 375-500 °C, respectively,
461 whilst PU decomposed between 225°C-500 °C. The PE/PU/PET film

462 decomposed primarily between 350-500 °C. As expected in PE/PU/PET and
463 Layer A (PE + PU), there was a small mass loss between 200 °C to 400 °C,
464 related to the PU decomposition. In contrast, weight loss in this range for layer B
465 was negligible, confirming the absence of PU.

466 The DSC thermogram of an MDO-PE film in **Figure 6** showed two endothermic
467 peaks between 120 and 135 °C. These two melting peaks indicated the presence
468 of two different crystalline domains in MDO-PE: one less ordered with a T_m similar
469 to Linear Low Density Polyethylene (LLDPE, $T_m = 125$ °C) and the other at a
470 higher temperature ($T_m = 133$ °C) associated with oriented PE domains [40]. The
471 double peak may be related to the multilayer structure of this film.

472



473

474 **Figure 6.** DSC thermograms of MDO-PE/PU/PE and MDO-PE films and the
475 layers obtained after the CO₂ + methanol treatment, indicating the different T_m
476 transitions.

477

478 The same transitions were observed in the MDO-PE/PU/PE film and the
479 delaminated layer A (MDO-PE). The relative intensity of the two peaks was,
480 however, different. In the MDO-PE/PU/PE film, the peak at higher temperature
481 was weaker due to the lower percentage of MDO-PE in the composite material.
482 Comparison of the thermograms of layer A and MDO-PE showed the same
483 transitions, although the relative intensity of the second melting peak at the
484 elevated temperature was slightly lower in layer A than in pure MDO-PE. This

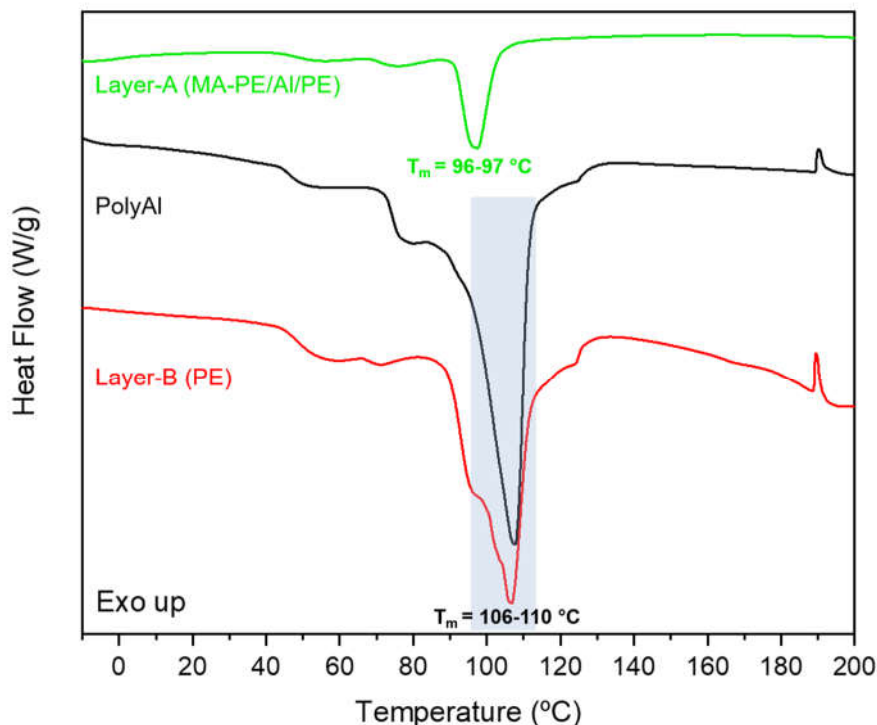
485 suggests that the delamination process was not clean. In contrast, DSC of layer
486 B showed only a single endothermic peak at 125 °C that corresponded to LLDPE
487 [40].

488 The exothermic peak at approximately 175 °C was only present in the
489 thermograms of multilayer MDO-PE/PU/PE and layer MDO-PE/PU.

490 The T_g of PU was not evident in any of the thermograms. PE and MDO-PE in
491 both single-component and MDO-PE/PU/PE multilayer films started to melt at
492 room temperature.

493 In the case of the PolyAl system, DSC thermograms of the composite system
494 before treatment and the delaminated layers are compared in **Figure 7**.
495 Regarding PolyAl, a broad endothermic peak was observed between 106-110 °C.
496 This low melting point is in accordance with the melting point of LDPE [40]. This
497 peak was also observed in the delaminated layer B (PE). A similar endothermic
498 peak was observed in layer A but shifted to 96-97 °C. The lower melting point
499 could be related to the carboxylic acid groups present in the MA-PE. This is in
500 agreement with the FTIR results. Once more, there is an exothermic peak, this
501 time at 190 °C, which may be attributed to fillers or additives incorporated into the
502 composite material.

503



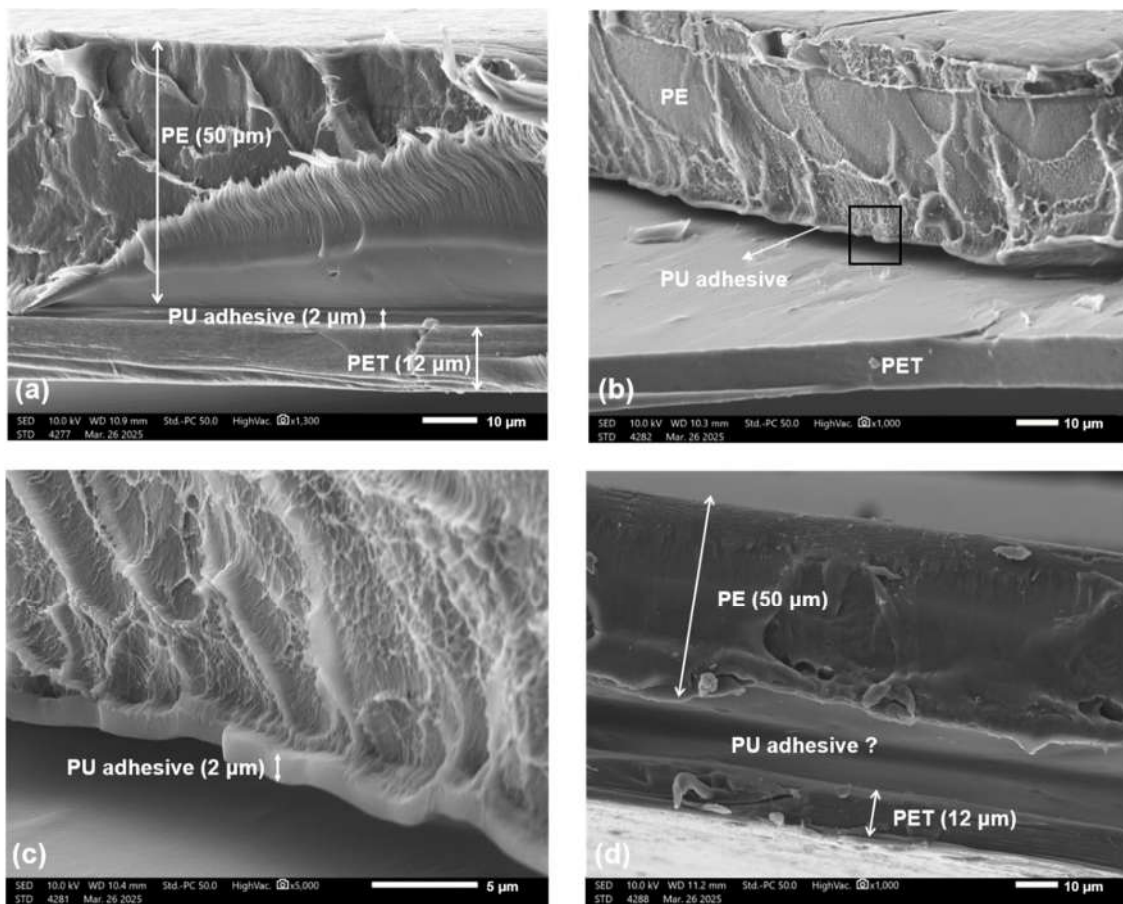
504

505 **Figure 7.** DSC thermogram of PolyAl multilayer film and the layers obtained after
506 the CO₂ + methanol treatment, indicating the different T_m transitions.

507

508 **Figure 8** presents SEM micrographs of the commercial PE/PU/PET sample,
509 where the distinct PE, PU, and PET layers can be clearly identified with
510 thicknesses of approximately 50, 2, and 12 μm , respectively (Figures 8a, 8c, and
511 8d). These values are consistent with the specifications provided by the
512 manufacturer. During SEM sample preparation, a slight separation between the
513 PET and PU layers occurred as a result of the freeze-fracture procedure (Figure
514 8a). In contrast, **Figure 8d** shows a sample delaminated with CO_2 . The film
515 thickness of the PE and PET films remained unchanged after CO_2 delamination,
516 whilst PU adhesive was not clearly observed.

517



518

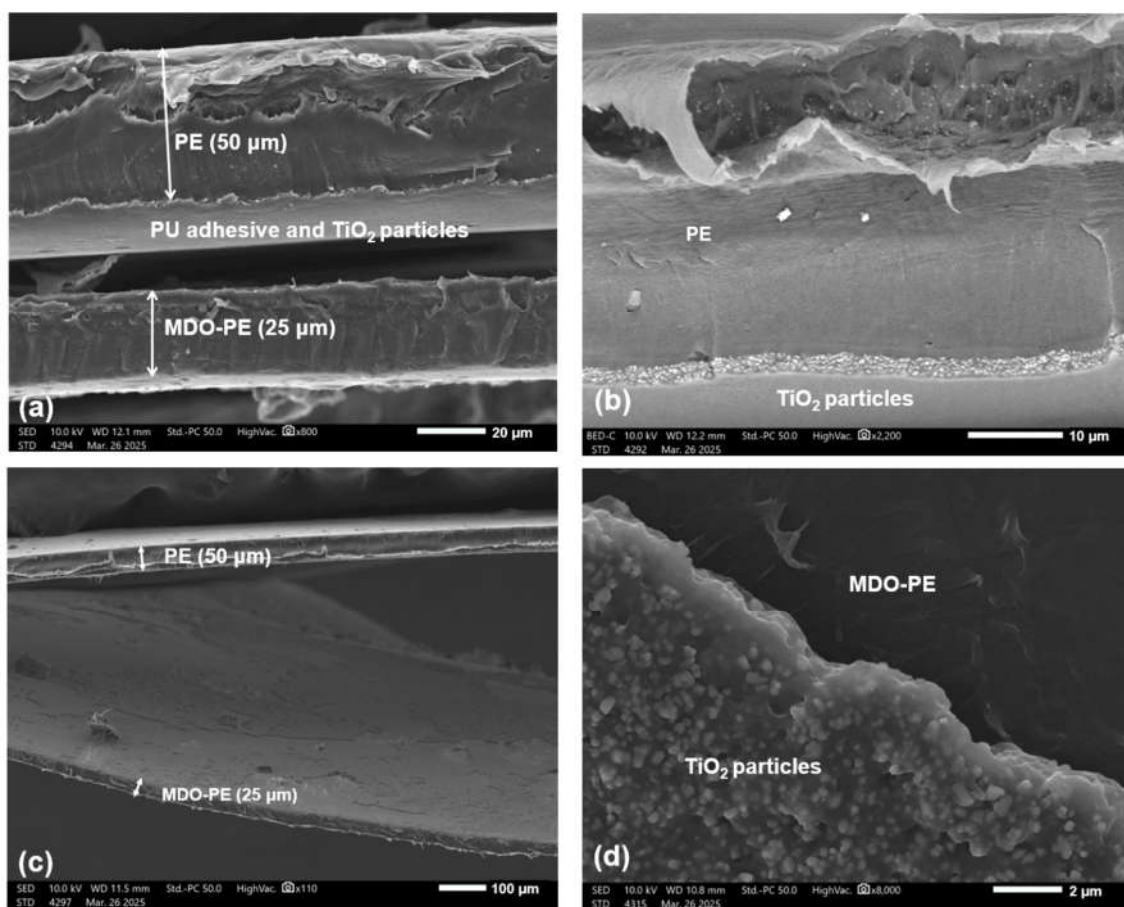
519 **Figure 8.** SEM images of: (a) PE/PU/PET film fractured using liquid N_2 , (b) region
520 delaminated due to liquid N_2 where PE, PU and PET are distinguished, (c) a
521 closer view (black square in (b)) near the delamination place (PE/PU above and
522 PET below) showing the PU adhesive, and (d) PE/PU/PET delaminated film after
523 the CO_2 + methanol treatment.

524

525 SEM images for the MDO-PE/PU/PE film are shown in **Figure 9**. During sample
526 preparation for SEM by freezing fracture, delamination occurred, resulting in a

527 thicker layer (PE) and a thinner layer (MDO-PE). The thickness measurements
528 in **Figure 9a** matched well the values provided by the company.

529



530

531 **Figure 9.** SEM images of: (a) MDO-PE/PU/PE film fractured using liquid N₂
532 (slightly delaminated), (b) back Scattering image of the PE layer in the MDO-
533 PE/PU/PE multilayer film showing TiO₂ nanoparticles, (c) MDO-PE/PU/PE
534 delaminated system after the CO₂ + methanol treatment, and (d) a front view of
535 the MDO-PE delaminated layer.

536

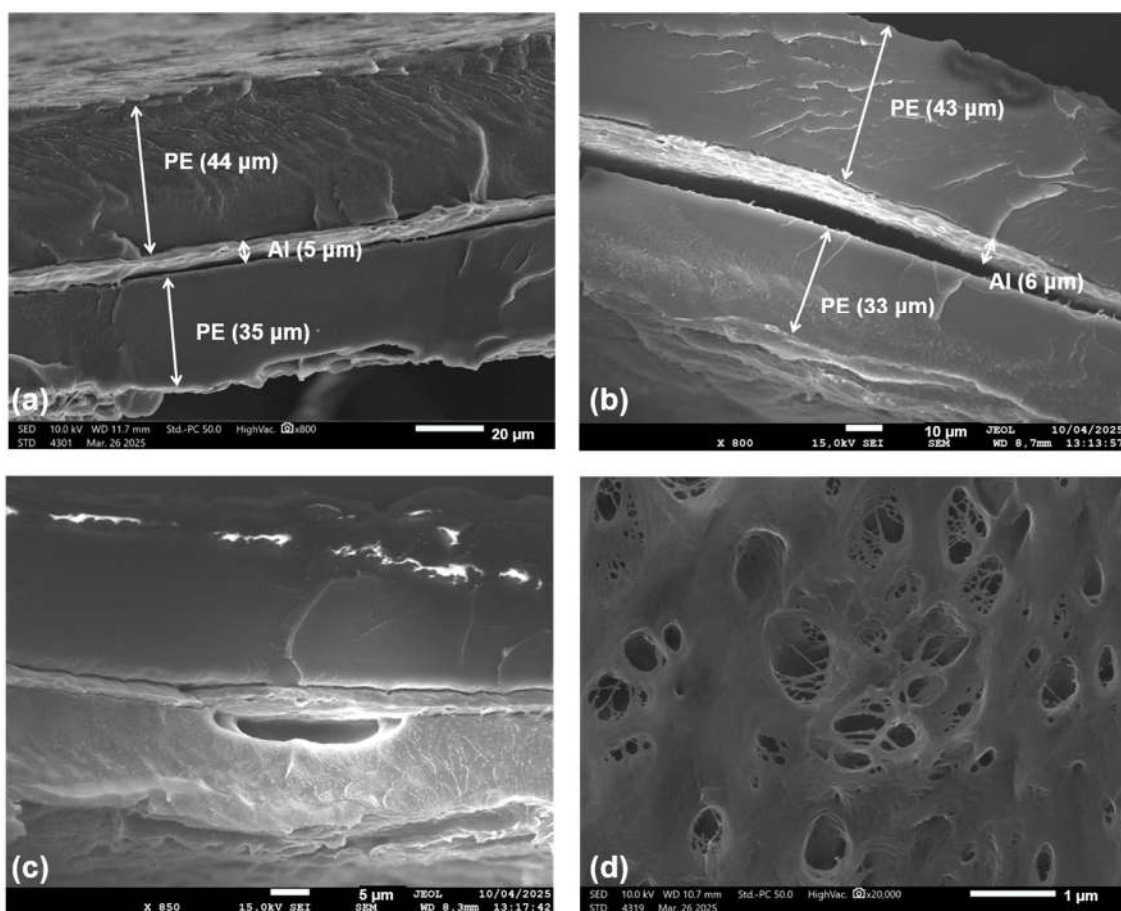
537 Small and bright spherical particles were observed in the SEM images of the
538 MDO-PE/PU/PE film. EDX analysis allowed their identification as TiO₂
539 (Supplementary Material, **Figure S4**). TiO₂ particles were used to provide the
540 white colour to the PE film. Although the TiO₂ particles were originally introduced
541 in the internal part of the PE film, SEM images showed that during lamination,
542 particles migrated to the PU layer (**Figure 9b**).

543 SEM images of the CO₂ delaminated material are also presented in **Figure 9c**
544 and **9d**, clearly showing the PE and MDO-PE layers. A close inspection of the
545 inner face of the MDO-PE layer after delamination showed the presence of
546 domains formed by TiO₂ particles, indicating that delamination took place at the

547 TiO₂/PU layer interface but not in a clean way. Similarly, SEM images of the PE
548 inner layer revealed the presence of TiO₂ nanoparticles embedded into a polymer
549 matrix. Thus, during delamination in CO₂, TiO₂ particles and PU were distributed
550 between both layers.

551 These results agree with the ATR-FTIR results in **Figure 3c**. The spectra of the
552 inner surfaces of both delaminated layers exhibited characteristic PU signals and
553 a broad band starting at 700 cm⁻¹, attributed to TiO₂. It is worth noting that the
554 MDO-PE layer appears slightly pink due to TiO₂ residues retained on the
555 magenta-printed surface (see **Figure 3a**).

556



557

558 **Figure 10.** SEM images of: (a) PolyAl film fractured using liquid N₂, (b) PolyAl
559 delaminated system after the CO₂ + methanol treatment, (c) localised
560 delamination site (bubble) observed between the Al and PE layers, (d) a front
561 view of the MA-PE layer.

562

563 **Figure 10** shows SEM images of the PolyAl samples. In the untreated PolyAl
564 sample (**Figure 10a**), at least three different layers were identified (one Al layer
565 between two PE layers). **Figure 10b** shows an SEM image of the sample after
566 the CO₂ treatment. The thickness of the layers remains almost the same before

567 and after the CO₂ treatment. **Figure 10c** highlights a possible delamination site
 568 in the form of a bubble. **Figure 10d** shows a front view of the MA-PE layer after
 569 delamination (CO₂ treatment), where several “bubble holes” are spread along the
 570 surface. This fact demonstrates that there is a mechanical modification of the film
 571 before delamination.

572 It is interesting to note that, during sample preparation for SEM, most samples
 573 partially delaminated during fracture at the same interface as samples
 574 delaminated with CO₂, which evidenced that delamination always took place at
 575 the weakest interface.

576

577 **3.3. Delamination of commercial multilayer polymer films with scCO₂ and** 578 **different cosolvents**

579

580 Further experiments were conducted using additional cosolvents besides
 581 methanol, including ethanol, acetone, DMSO, and water. The amount of
 582 cosolvent was always equal to 5 mL, that is 8.3 % in volume and corresponds to
 583 mass percentages between 10.7 and 10.8% for acetone, methanol and ethanol,
 584 13.3% for water and 14.5% for DMSO. The approximate mass calculation was
 585 performed, considering the volume of the reactor and the density of CO₂ at 80 °C
 586 and 200 bar and neglecting the volume of mixing. At 80 °C and 200 bar the CO₂
 587 + organic cosolvent system remained in the one-phase region [36, 37, 42-45].
 588 However, the solubility of water in CO₂ was much lower than the amount added.
 589 In particular, at 80 °C and 200 bar, it is close to 0.75 % mass [46]. The presence
 590 of cosolvents is expected to change the swelling of the polymers as compared to
 591 pure CO₂. **Table 2** summarises the results.

592 A qualitative comparison of the cosolvent effect was performed, establishing a
 593 scale ranging from 1 to 4, meaning: (1) no delamination or visible separation
 594 between layers, (2) slight delamination with partial interfacial weakening
 595 observed; layers can only be minimally separated at the edges or with external
 596 force, (3) moderate delamination with a clear separation over a significant portion
 597 of the interface; delamination can be manually extended with moderate effort, but
 598 some adhesion zones remain, (4) complete delamination leading to full interfacial
 599 separation; layers detach easily and cleanly with minimal force (e.g., tweezers).

600 **Table 2.** Delamination degree of the different films with CO₂ modified by different
 601 cosolvents, ranging from (1) no delamination, (2) slight (minimal, edge-limited),
 602 (3) moderate (partial, extended), (4) complete delamination.

	PE/PU/PET	MDO-PE/PU/PE	PolyAl
DMSO	4	4	4
methanol	4	4	3
ethanol	4	3	1

acetone	2	2	1
water	2	1	1

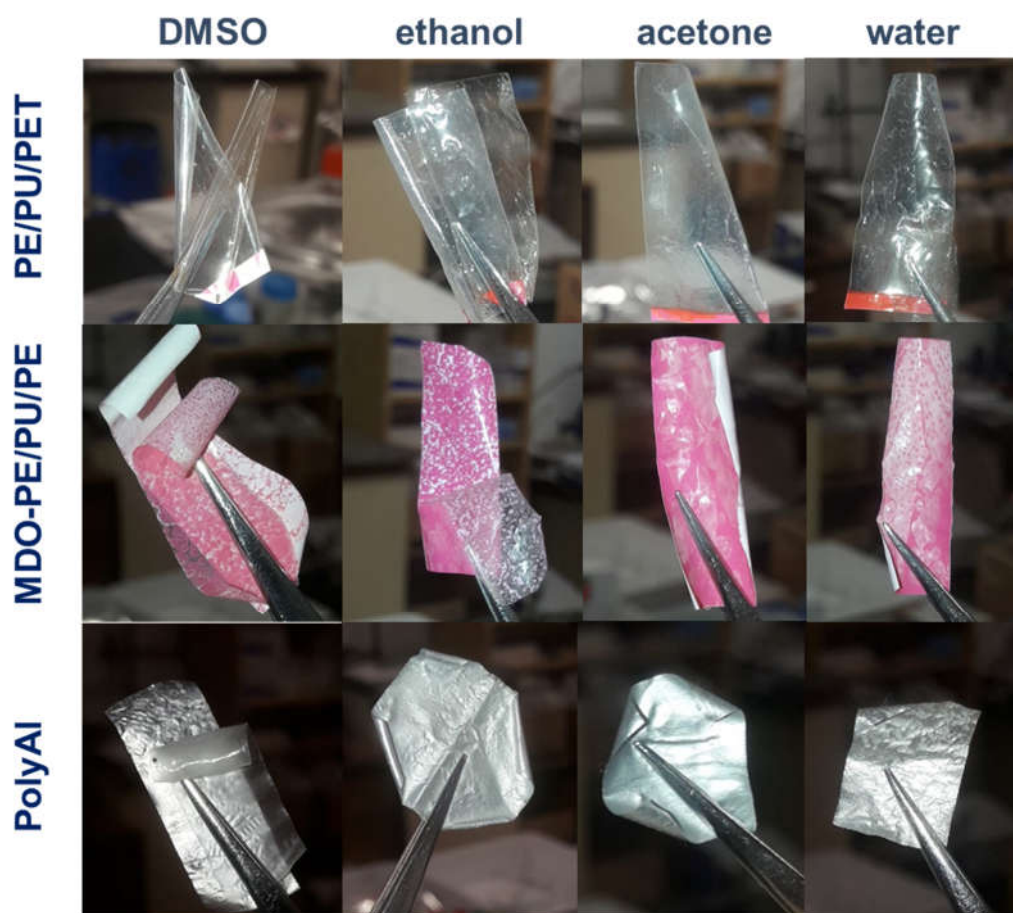
603

604 The degree of delamination varied with the cosolvent and the multilayer film.
 605 DMSO was the best cosolvent for the CO₂ delamination of all films. Methanol was
 606 also a good cosolvent. The higher delamination efficiency of DMSO can be
 607 partially related to its higher mass concentration in the experiments. DMSO is
 608 highly soluble in CO₂. Although it has the highest boiling point of all cosolvents
 609 used ($T_m = 189$ °C), it could be very easily recovered from the CO₂ stream by
 610 distillation with near-complete recovery, as demonstrated for the separation of
 611 ethyl acetate-CO₂ [47]. Therefore, both CO₂ and the cosolvent could be efficiently
 612 recycled in a simple loop. CO₂ would only require recompression and thermal
 613 adjustment to restore process conditions. Moreover, DMSO is classified as a
 614 Class 3 solvent according to ICH (International Council for Harmonisation)
 615 guidelines, indicating low toxicological concern and enabling broader application
 616 in environmentally responsible processes.

617 In contrast, acetone and water were bad cosolvents. Ethanol behaved differently
 618 for each system; it helped in the delamination of PE/PU/PET and MDO-
 619 PE/PU/PE, but not for PolyAl. In systems where both methanol and ethanol
 620 successfully promoted delamination, ethanol would be a more suitable cosolvent
 621 due to its lower toxicity (Class 3 vs. Class 2), despite its generally higher industrial
 622 cost, particularly in its non-denatured form, owing to production methods and
 623 taxation. **Figure 11** shows images of the films delaminated using CO₂ and the
 624 four additional cosolvents.

625 Miscibility of the polymers and cosolvents was studied using the Hansen theory
 626 [48]. The Hansen solubility parameters calculated from the dispersion, polar and
 627 H-bonding forces (shown in **Tables S1** and **S2**, Supplementary Material)
 628 indicated that acetone was the best solvent for PU and PET (slightly worse for
 629 PET). DMSO was also a good solvent for PU and PET. In contrast, acetone and
 630 DMSO were bad solvents for PE. Methanol, ethanol, and water were bad solvents
 631 for all the polymers, water being the worst. Although water and alcohols are bad
 632 solvents for the polymers involved, they are protic solvents, which could promote
 633 the hydrolysis of PU. In the case of water, despite being a protic solvent, it may
 634 have failed in the delamination due in part to its low solubility in scCO₂. The fact
 635 that there is no correlation between the mutual solubility of the polymer and the
 636 cosolvent and the delamination behaviour, strengthens the role of CO₂ in the
 637 process.

638



639

640 **Figure 11.** Images of the commercial films delaminated using CO₂ modified with
 641 the different cosolvents. Sample size for PE/PU/PET and MDPO-PE/PU/PE and
 642 PolyAl (DMSO) ca. 3 x 1 cm² and for PolyAl (ethanol, acetone, water) 1.5-1.0 x
 643 1.5 cm².

644 In summary, although the treatment of a PET/PU multilayer material prepared in
 645 the lab with pure CO₂ followed by sudden depressurisation led to the separation
 646 of the PET and PU layers, successful delamination of other commercial and
 647 complex multilayer films was only possible when organic cosolvents were used.
 648 However, the success in the delamination using CO₂ and cosolvents did not
 649 follow the expected trend considering the mutual solubility of the polymers and
 650 cosolvents, so additional effects may take place.

651 The effluents of the delamination from PE/PU/PET films in pure CO₂ and CO₂
 652 modified with DMSO were collected in deuterated DMSO. ¹H NMR of the samples
 653 (**Figure S5**, Supplementary Material) showed minor bands at 1.2 ppm, ascribed
 654 to aliphatic CH₂ groups. Due to the extremely low solubility of PE in CO₂ [49],
 655 these bands may indicate the extraction by CO₂ of oligomers, additives,
 656 polymerisation aids or unintended added substances present in the films [50]. No
 657 aromatic signals between 6.5 and 8.0 ppm due to PET or PU monomers or
 658 oligomers were observed.

659 Thus, we propose for the CO₂ delamination process a multiple mechanism
660 involving (1) the generation of mechanical stress induced by the sorption of CO₂
661 into the polymers and preferential polymer swelling, followed by the sudden
662 depressurisation, (2) the selective dissolution of the adhesive or the weakening
663 of interfacial interactions between polymers induced by cosolvents. Previous
664 research indicates that at higher temperatures, foaming of the polymers at the
665 interface could also induce delamination [23, 24]. We envision that the separation
666 between the PE layer and the PU adhesive using CO₂ may be possible by
667 employing different conditions. The technique can also be combined with other
668 physical or chemical recycling processes. Further studies are required to
669 elucidate the exact delamination mechanism in CO₂ to be able to extend the
670 process to other complex multilayer materials of interest.

671

672 **4. CONCLUSIONS AND OUTLOOK**

673 A new delamination process for multilayer plastics using supercritical CO₂ was
674 demonstrated as a promising and sustainable alternative to current recycling
675 technologies. Given the increasing concern around the environmental impact and
676 technical challenges of recycling these materials, there is an urgent need for
677 innovative approaches that are efficient, scalable, and environmentally friendly.

678 As a proof of concept, three commercial multilayer films, PE/PU/PET, MDO-
679 PE/PU/PE and PolyAl, were treated using supercritical CO₂ at 80 °C and 200 bar
680 in the presence of various cosolvents, followed by rapid depressurisation.
681 Selective delamination mainly occurred at the adhesive interfaces, depending on
682 film composition. ATR-FTIR, DSC, and SEM analyses confirmed the release of
683 distinct polymer layers.

684 Differences in the delamination efficiency were observed among the cosolvents
685 used. DMSO and methanol showed the highest delamination efficiency,
686 particularly at the PU-based adhesive interfaces, while acetone and water were
687 ineffective under the tested conditions. DMSO is preferred due to its lower toxicity
688 and the ease with which it can be separated from CO₂ by distillation for
689 subsequent recycling.

690 A general mechanism for the CO₂ delamination process is proposed, considering
691 both mechanical and chemical effects. The different degree of swelling induced
692 by scCO₂ and the cosolvents in the polymers, followed by rapid depressurisation,
693 can cause mechanical stress and/or foaming, promoting delamination. The
694 selective dissolution of the adhesive or weakening of the interaction at the
695 interface caused by the cosolvents is also possible.

696 Further investigation is needed to fully understand the delamination mechanism
697 and enable broader application to other multilayer materials. Using several cycles
698 sequentially at the same or different conditions could allow the delamination of

699 complex multilayer materials. Solvent-based methods show the highest
700 delamination efficiency but carry the highest environmental and disposal
701 concerns. Mechanical and thermal methods are simple but limited in efficiency
702 and compatibility. The scCO₂ method combines the advantages of physical and
703 chemical methods at less aggressive conditions, reducing substantially the
704 amount of organic solvent used.

705 Furthermore, the scCO₂ method aligns with key principles of Green Chemistry,
706 such as the use of safer solvents and waste prevention. It also complies with
707 energy efficiency due to the mild operation conditions and simple sample
708 recovery. Furthermore, it offers added benefits, such as the possible extraction of
709 CO₂-soluble contaminants and the potential sterilisation of post-consumer waste
710 plastics simultaneously with the separation process.

711 We are currently studying the effect of the sample size and mechanical stirring in
712 the delamination process. After delamination, a density-based separation of the
713 polymers could be performed. The method still requires optimisation, and a full
714 life cycle assessment must be conducted to evaluate its environmental
715 performance. However, given its mild operating conditions and important process
716 advantages, the process holds strong potential for scale-up. Notably, numerous
717 supercritical CO₂-based technologies have already been implemented at
718 commercial scale under similar conditions. Engineering know-how and industrial
719 expertise in supercritical fluid processing are well established, and several
720 specialised companies could readily design and construct large-scale
721 installations. If validated, this technology could help shift the paradigm in plastic
722 recycling and contribute meaningfully to a more circular, sustainable economy.

723

724 **ACKNOWLEDGEMENTS**

725 The authors acknowledge funding from MICIU project PID2022-137847OB-10.
726 We thank R. Ciganda from Plastigaur S.A. (Spain) for kindly providing the
727 multilayer samples, Prof. E. Enciso at UCM for the use of ATR-FTIR and Prof. J.
728 González-Benito at the University Carlos III of Madrid for useful discussion. We
729 acknowledge the ICTS National Microscopy Centre and the Chemical
730 Technologies CAI at UCM and their staff for the use of the technical facilities.

731

732 **REFERENCES**

- 733 [1] J.-P. Lange, Managing plastic waste-Sorting, recycling, disposal, and product
734 redesign, ACS. Sustainable Chem. Eng., 9 (2021) 15722-15738.
735 [2] A. Schade, M. Melzer, S. Zimmermann, T. Schwarz, K. Stoewe, H. Kuhn,
736 Plastic waste recycling—A chemical recycling perspective, ACS. Sustainable
737 Chem. Eng., 12 (2024) 12270-12288.
738 [3]<https://plasticseurope.org/knowledge-hub/plastics-the-fast-facts-2023/>

739 [4] E. Barnard, J.J. Rubio Arias, W. Thielemans, Chemolytic depolymerisation of
740 PET: A review, *Green Chem.*, 23 (2021) 3765-3789

741 [5] F. Xie, Biopolymer-based multilayer films and coatings for food preservation:
742 an update of the recent development, *Curr. Food Sci. Technol. Rep.*, 1 (2023) 1-
743 12.

744 [6] M. Seier, V.M. Archodoulaki, T. Koch, B. Duscher, M. Gahleitner, Prospects for
745 recyclable multilayer packaging: A case study, *Polymers*, 15 (2023) 2966.

746 [7] P. Tamizhdurai, V.L. Mangesh, S. Santhosh, R. Vedavalli, C. Kavitha, J.K.
747 Bhutto, M.A. Alreshidi, K.K. Yadav, R. Kumaran, A state-of-the-art review of
748 multilayer packaging recycling: Challenges, alternatives, and outlook, *J. Cleaner*
749 *Prod.*, 447 (2024) 141403,.

750 [8] J. Guan, Z. Dai, R. Wang, C. Zhang, S. Chen, Y. Guo, X. Zhang, Y. Wu,
751 Pollution characteristics and control strategies of typical waste plastic recycling
752 plants, *J. Environ. Chem. Eng.*, 13 (2025) 116398.

753 [9] K.M. Patel, M.M. Vaviya, M.H. Patel, Process for recovering low-density
754 polyethylene from flexible packaging material, WO 2015/159301 A3, 2015.

755 [10] A. Mukhopadhyay, Process of Delamination of Multi-layer Laminated
756 Packaging Industrial Refuse, US 2004/0054018 A1, 2004.

757 [11] M. Fraldi, A. Cutolo, L. Esposito, G. Perrella, M.G. Pastore Carbone, L.
758 Sansone, G. Scherillo, G. Mensitieri, Delamination onset and design criteria of
759 multilayer flexible packaging under high pressure treatments, *Innovative Food*
760 *Sci. Emerg. Technol.*, 23 (2014) 39-53.

761 [12] G.L. Robertson, Recycling of Aseptic Beverage Cartons: A Review,
762 *Recycling*, 6 (2021) 20.

763 [13] A. Preetam, P.R. Jadhao, S.N. Naik, K.K. Pant, V. Kumar, Supercritical fluid
764 technology - an eco-friendly approach for resource recovery from e-waste and
765 plastic waste: A review, *Sep. Purif. Technol.*, 304 (2023) 122314.

766 [14] D.L. Tomasko, H. Li, D. Liu, X. Han, M.J. Wingert, L.J. Lee, K.W. Koelling, A
767 review of CO₂ applications in the processing of polymers, *Ind. Eng. Chem. Res.*,
768 42 (2003) 6431-6456.

769 [15] C.S. Castro Issasi, M. Sasaki, A.T. Quitain, T. Kida, N. Taniyama, Removal
770 of impurities from low-density polyethylene using supercritical carbon dioxide
771 extraction, *J. Supercrit. Fluid.*, 146 (2019) 23-29.

772 [16] A. Alassali, N. Aboud, K. Kuchta, P. Jaeger, A. Zeinolebadi, Assessment of
773 Supercritical CO₂ Extraction as a Method for Plastic Waste Decontamination,
774 *Polymers*, 12 (2020) 1347.

775 [17] H.K. Ruiz, J.M. Gómez-Salazar, L. Calvo, A. Cabañas, Characterisation of
776 plastic-based sanitary personal protective equipment following supercritical CO₂
777 sterilisation: A reuse strategy, *J. CO₂. Util.*, 92 (2025) 103029.

778 [18] G.B. Jacobson, L. Williams, W. Kirk Hollis, J. Barton, Craig M. V. Taylor,
779 SCORR - Supercritical Carbon Dioxide Resist Removal, in,
780 <https://www.osti.gov/servlets/purl/789412>, 2005, pp. 14004.

781 [19] J.W. King, L.L. Williams, Utilization of critical fluids in processing
782 semiconductors and their related materials, *Curr. Opin. Solid State Mater. Sci.*, 7
783 (2003) 413-424.

784 [20] C. Aymonier, C. Slostowski, Method and device for dismantling multilayer
785 systems including at least one organic component, WO2017/037260A1, 2016.

786 [21] A. Briand, A. Leybros, C. Audoin, J.C. Ruiz, F. Lamadie, A. Grandjean, CO₂
787 absorption into a polymer within a multilayer structure: The case of poly(ethylene-
788 co-vinyl acetate) in photovoltaic modules, *J. Supercrit. Fluid.*, 179 (2022).

789 [22] A. Briand, A. Leybros, O. Doucet, J.-C. Ruiz, P. Fontaine-Giraud, L. Liotaud,
790 A. Grandjean, Versatility assessment of supercritical CO₂ delamination for
791 photovoltaic modules with ethylene-vinyl acetate, polyolefin or ethylene
792 methacrylic acid ionomer as encapsulating polymer, *J. Cleaner Prod.*, 410 (2023)
793 137292.

794 [23] A. Briand, A. Leybros, O. Doucet, M. Vite, A. Gasmi, J.C. Ruiz, F. Lamadie,
795 A. Grandjean, Deformation-induced delamination of photovoltaic modules by
796 foaming ethylene-vinyl acetate with supercritical CO₂, *J. CO₂. Util.*, 59 (2022).

797 [24] J.L. Sumei, J.A. Sarver, E. Kiran, Foaming of polystyrene and poly(methyl
798 methacrylate) multilayered thin films with supercritical carbon dioxide, *J.*
799 *Supercrit. Fluid.*, 145 (2019) 243-252.

800 [25] R.K. Sharma, Y. Mori, S. Kishimoto, T. Kida, K. Tokumitsu, T. Sato, K.
801 Yoshimoto, K. Taki, Sustainable approach for recycling metal–polymer
802 composites using foaming technology, *Chem. Eng. J.*, 512 (2025) 162349.

803 [26] D. Mu, J. Liang, J. Zhang, Y. Wang, S. Jin, C. Dai, Exfoliation of Active
804 Materials Synchronized with Electrolyte Extraction from Spent Lithium-Ion
805 Batteries by Supercritical CO₂, *ChemistrySelect*, 7 (2022) e202200841.

806 [27] N. Hayagan, C. Aymonier, L. Croguennec, C. Faure, J.-B. Ledeuil, M.
807 Morcrette, R. Dedryvère, J. Olchowka, G. Philippot, Direct Recycling Process
808 Using Pressurized CO₂ for Li-Ion Battery Positive Electrode Production Scraps,
809 *ACS. Sustainable Chem. Eng.*, 13 (2025) 105-118.

810 [28] J. González, E. Pérez, M. Pepczynska, L. Calvo, A. Cabañas, Supercritical
811 Solution Impregnation of naproxen into mesoporous SiO₂ SBA-15, *J. CO₂. Util.*,
812 73 (2023) 102518.

813 [29] C.K. Samios, K.G. Gravalos, N.K. Kalfoglou, In situ compatibilization of
814 polyurethane with poly(ethylene terephthalate), *Eur. Polym. J.*, 36 (2000) 937-
815 947.

816 [30] B. Das, D. Chakrabarty, C. Guha, S. Bose, Effects of corona treatment on
817 surface properties of co-extruded transparent polyethylene film, *Polym. Eng. Sci.*,
818 61 (2021) 1449-1462.

819 [31] M. Champeau, J.M. Thomassin, C. Jérôme, T. Tassaing, In situ FTIR micro-
820 spectroscopy to investigate polymeric fibers under supercritical carbon dioxide:
821 CO₂ sorption and swelling measurements, *J. Supercrit. Fluid.*, 90 (2014) 44-52.

822 [32] J. von Schnitzler, R. Eggers, Mass transfer in polymers in a supercritical
823 CO₂-atmosphere, *J. Supercrit. Fluid.*, 16 (1999) 81-92.

824 [33] Y.-T. Shieh, J.-H. Su, G. Manivannan, P.H.C. Lee, S.P. Sawan, W. Dale Spall,
825 Interaction of supercritical carbon dioxide with polymers. I. Crystalline polymers,
826 *J. Appl. Polym. Sci.*, 59 (1996) 695-705.

827 [34] S.A.E. Boyer, M.-H. Klopffer, J. Martin, J.-P.E. Grolier, Supercritical gas–
828 polymer interactions with applications in the petroleum industry. Determination of
829 thermophysical properties, *J. Appl. Polym. Sci.*, 103 (2007) 1706-1722.

830 [35] D. Hu, L. Yan, T. Liu, Z. Xu, L. Zhao, Solubility and diffusion behavior of
831 compressed CO₂ in polyurethane oligomer, *J. Appl. Polym. Sci.*, 136 (2019)
832 47100.

833 [36] A.-D. Leu, S.Y.K. Chung, D.B. Robinson, The equilibrium phase properties of
834 (carbon dioxide + methanol), *J. Chem. Thermodyn.*, 23 (1991) 979-985.

835 [37] K. Tochigi, T. Namae, T. Suga, H. Matsuda, K. Kurihara, M.C. dos Ramos, C.
836 McCabe, Measurement and prediction of high-pressure vapor–liquid equilibria for
837 binary mixtures of carbon dioxide+n-octane, methanol, ethanol, and
838 perfluorohexane, *J. Supercrit. Fluid.*, 55 (2010) 682-689.

839 [38] S. El-Sherbiny, F. Morsy, M. Samir, O.A. Fouad, Synthesis, characterization
840 and application of TiO₂ nanopowders as special paper coating pigment, Appl.
841 Nanosci., 4 (2014) 305-313.

842 [39] M. Haurat, T. Tassaing, M. Dumon, FTIR in situ measurement of swelling and
843 CO₂ sorption in acrylic polymers at high CO₂ pressures, J. Supercrit. Fluid., 182
844 (2022) 105534.

845 [40] G. Kaiser, S. Schmölder, C. Straßer, S. Pohland, S. Turan, Netzsch-
846 Gerätebau-GmbH, Handbook DSC: Differential Scanning Calorimetry, Netzsch-
847 Gerätebau GmbH, 2020.

848 [41] D.F. Baldwin, M. Shimbo, N.P. Suh, The Role of Gas Dissolution and Induced
849 Crystallization During Microcellular Polymer Processing: A Study of Poly
850 (Ethylene Terephthalate) and Carbon Dioxide Systems, J. Eng. Mater. Technol.,
851 117 (1995) 62-74.

852 [42] C.J. Chang, K.-L. Chiu, C.-Y. Day, A new apparatus for the determination of
853 P-x-y diagrams and Henry's constants in high-pressure alcohols with critical
854 carbon dioxide, J. Supercrit. Fluid., 12 (1998) 223-237.

855 [43] H.-Y. Chiu, R.-F. Jung, M.-J. Lee, H.-M. Lin, Vapor-liquid phase equilibrium
856 behavior of mixtures containing supercritical carbon dioxide near critical region,
857 J. Supercrit. Fluid., 44 (2008) 273-278.

858 [44] Ž. Knez, M. Škerget, L. Ilič, C. Lütge, Vapor-liquid equilibrium of binary CO₂-
859 organic solvent systems (ethanol, tetrahydrofuran, ortho-xylene, meta-xylene,
860 para-xylene), J. Supercrit. Fluid., 43 (2008) 383-389.

861 [45] Y. Sato, N. Hosaka, K. Yamamoto, H. Inomata, Compact apparatus for rapid
862 measurement of high-pressure phase equilibria of carbon dioxide expanded
863 liquids, Fluid Phase Equilib., 296 (2010) 25-29.

864 [46] K. Tödheide, E.U. Franck, Das zweiphasengebiet und die kritische kurve im
865 system kohlendioxid-wasser bis zu ddrucken von 3500 bar, Z. Phys. Chem., 37
866 (1963) 387-401.

867 [47] D.F. Tirado, A. Cabañas, L. Calvo, Modelling and scaling-up of a supercritical
868 fluid extraction of emulsions process, Processes, 11 (2023) 1063.

869 [48] S. Abbott, C.M. Hansen, H. Yamamoto, Hansen Solubility parameters in
870 practice – Complete with software, data, and examples, 5th ed., 2015.

871 [49] C.F. Kirby, M.A. McHugh, Phase behavior of polymers in supercritical fluid
872 Solvents, Chem Rev., 99 (1999) 565-602.

873 [50] B.S. Anouar, C. Guinot, J.-C. Ruiz, F. Charton, P. Dole, C. Joly, C. Yvan,
874 Purification of post-consumer polyolefins via supercritical CO₂ extraction for the
875 recycling in food contact applications, J. Supercrit. Fluid., 98 (2015) 25-32.

876

Supplementary Material

Sustainable Delamination of Multilayer Plastic Films for Advanced Recycling

Ramiro J. Olmos-Greco¹, Eduardo Pérez¹, Lourdes Calvo², Albertina Cabañas^{1,*}

¹Department of Physical Chemistry, ²Department of Chemical Engineering and Materials, Complutense University of Madrid, 28040 Madrid, Spain

*Corresponding author's email: a.cabanas@quim.ucm.es

1. Structure of commercial multilayer films.

The commercial multilayer films provided by Plastigaur Company have several sub-layers. The arrangement is illustrated in **Figure S1**.

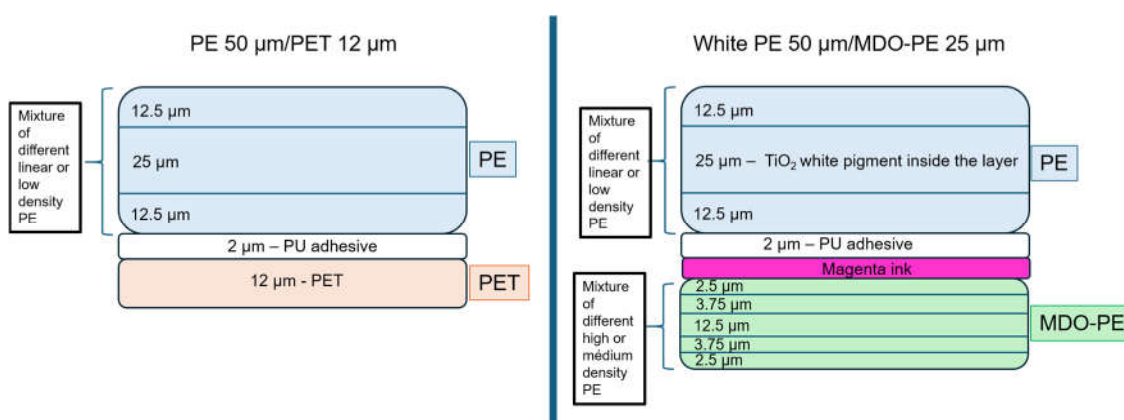


Figure S1. Multilayer structure of commercial films showing sub-layers: (a)PE/PU/PET and (b)PE/PU/MDO-PE system.

2. Thermogravimetric Analysis

TGA analysis of the PE/PU/PET multilayer films, the separated layers A and B (Table 1), and the PU adhesive prepared according to the vendor's instructions was also performed and is shown in **Figure S2**.

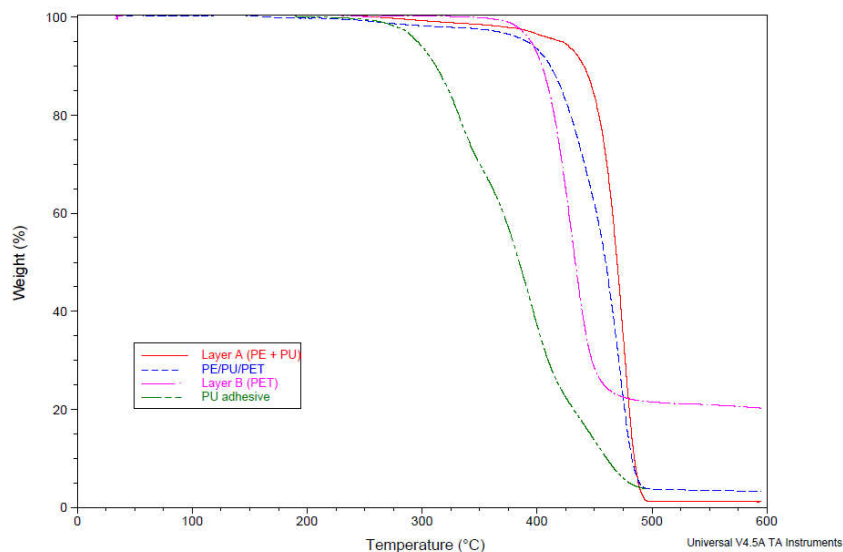


Figure S2. TGA analysis of the PE/PU/PET multilayer film, the separated layers: A (PE + PU) and B (PET) and the PU adhesive

Layer A (PE + PU) and layer B (PET) decomposed mostly between 420-500 °C and 375-500 °C, respectively, whilst PU decomposed between 225°C-500 °C. The PE/PU/PET film decomposed between 350-500 °C. As expected in PE/PU/PET and Layer A (PE + PU), there was a small mass loss between 200 °C to 400 °C, related with the PU decomposition. In contrast, weight loss in this range for layer B was negligible, confirming the absence of PU.

3. .PU Adhesive preparation (Morchem PL272A+CF-60)

The adhesive preparation was performed in the laboratory following the supplier's instructions. The polyurethane adhesive is formed by mixing the separate components: PL272A (the glue) and CF-60 (the hardener). The mixture ratio used was 100 to 70, respectively. Prior to the mixing process, the components were thermostated at 40 °C in a water bath. Then, 0.23 g of CF-60 was added using a 1 mL syringe to a 25 ml flask containing 0.32 g of PL272A, which had previously been weighed with a magnetic stirring bar. After that, stirring was initiated, and the temperature was maintained at 40 °C for 45-60 minutes. Finally, the mixture was placed in an oven at 50 °C for further drying and hardening for 24 hours.

The DSC of the PU adhesive prepared is shown in **Figure S3**. A T_g at ca. 5 °C was observed in the sample, followed by other minor and unclear thermal events.

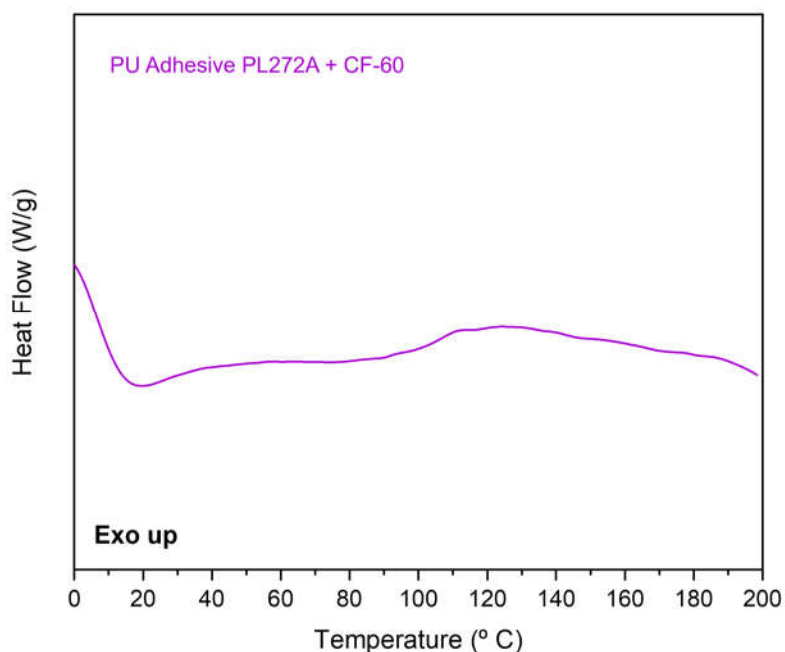
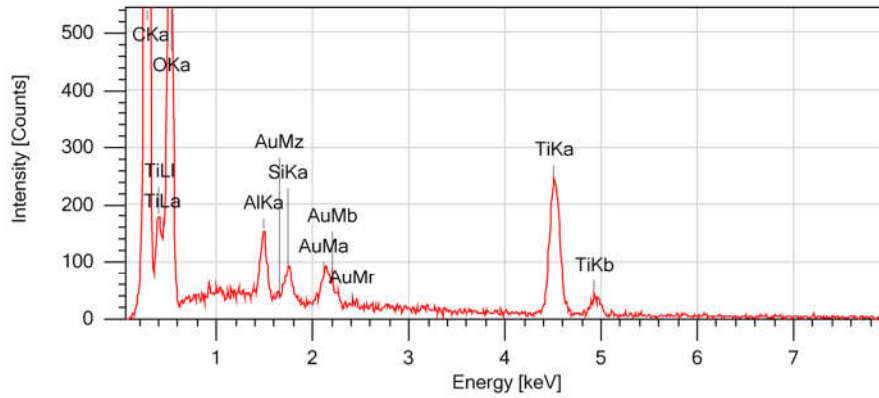
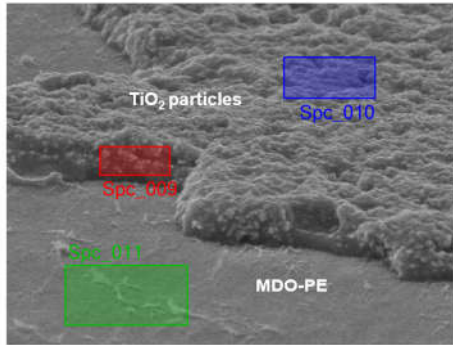


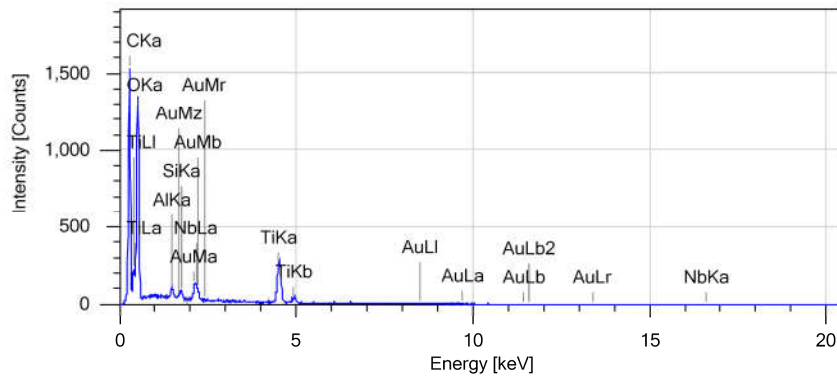
Figure S3. DSC thermogram of the adhesive prepared in the lab.

4. Characterisation of MDO-PE by EDX.

Energy-dispersive X-Ray spectroscopy (EDX) was conducted on the SEM images. **Figure S4** shows a SEM image and the spectra taken at three different locations. Analysis of the red and blue zones indicated the presence of Ti with a high mass percentage of ca. 24.8 % in both zones. Analysis of the green zone, however, did not show Ti. Therefore, titanium is present in the interphase zone of the laminates in a considerable quantity, as a different layer. This analysis confirms the identification of TiO_2 and the delamination place.



Element	Line	Mass%	Atom%
C	K	40.63±0.35	58.60±0.50
O	K	28.37±0.67	30.71±0.72
Al	K	1.45±0.11	0.93±0.07
Si	K	0.73±0.09	0.45±0.05
Ti	K	24.77±0.92	8.96±0.33
Au	M	4.05±0.33	0.36±0.03
Total		100.00	100.00
Spc_009			Fitting ratio 0.0334



Element	Line	Mass%	Atom%
C	K	31.32±0.30	47.87±0.46
O	K	35.62±0.69	40.87±0.79
Al	K	0.80±0.08	0.54±0.05
Si	K	0.72±0.08	0.47±0.05
Ti	K	24.68±0.87	9.46±0.33
Nb	L	1.45±0.22	0.29±0.04
Au	M	5.42±0.38	0.50±0.04
Total		100.00	100.00
Spc_010			Fitting ratio 0.0452

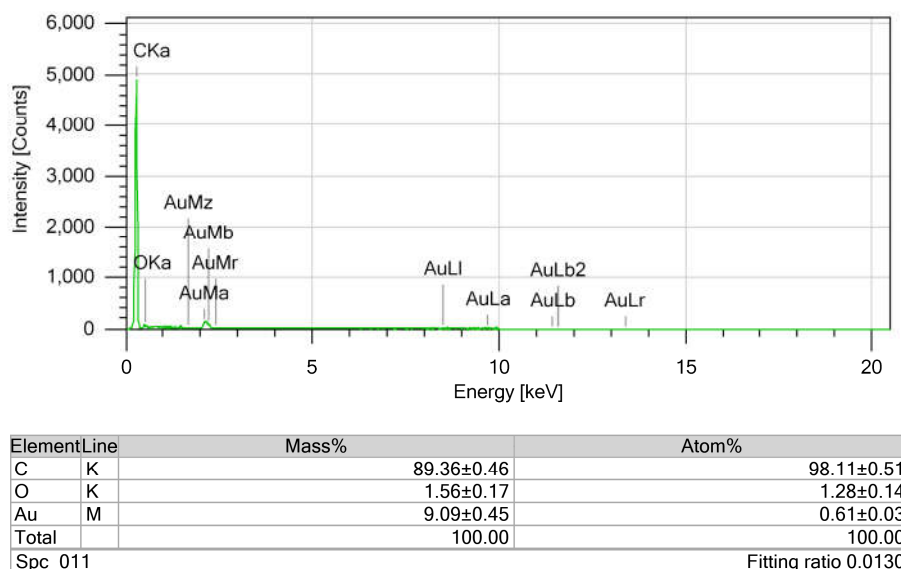


Figure S4. SEM image and EDX spectra of MDO-PE layer in three different zones (red, blue and green highlighted in the micrograph).

5. Hansen solubility parameters

Solubility of the cosolvents into the different polymers was studied using the Hansen solubility parameters (HSP) approach [1]. Table S1 shows the Hansen solubility parameters (δ_D , δ_P , δ_H) for the solvents and the polymers used in the calculation.

Table S1. Hansen solubility parameters for the solvents and polymers used in this study.

	δ_D (MPa ⁻¹)	δ_P (MPa ⁻¹)	δ_H (MPa ⁻¹)
MeOH	14.7	12.3	22.3
Water	15.5	16.0	42.3
Acetone	15.5	10.4	7.0
Ethanol	15.8	8.8	19.4
DMSO	18.4	16.4	10.2
PET	18.2	6.4	6.6
PE	16.0	0.8	2.8
PU	18.1	9.4	4.5

These parameters were used to calculate the parameter distance between two molecules, R_a , as the measurement of how alike they are according to (1). The smaller R_a , the more likely they are to be compatible.

$$R_a^2 = 4(\delta_{D1}-\delta_{D2})^2 + (\delta_{P1}-\delta_{P2})^2 + (\delta_{H1}-\delta_{H2})^2 \quad (1)$$

Table S2. R_a values of the different polymers and cosolvents

	R_a (acetone) (MPa ⁻¹)	R_a (ethanol) (MPa ⁻¹)	R_a (methanol) (MPa ⁻¹)	R_a (DMSO) (MPa ⁻¹)	R_a (water) (MPa ⁻¹)
PET	6.7	13.9	18.2	10.6	37.4
PE	10.5	18.4	22.8	17.9	42.3
PU	5.9	15.6	19.3	9.1	38.7

Solvents with R_a values lower than 10 (or close to this value) for a given polymer are considered good solvents. From the R_a values, only acetone and DMSO are considered good solvents for PU and PET (slightly worse for PET), whilst they are bad solvents for PE. The rest of the solvents are bad solvents for all the polymers, with water being the worst.

6. ¹H NMR analysis of the effluent

The effluents of the delamination from PE/PU/PET films in pure CO₂ and CO₂ modified with DMSO were collected in deuterated DMSO. ¹H NMR of the samples showed bands of the solvent DMSO (2.5 ppm) along with water (3.3 ppm) as an impurity, and in some samples bands of acetone (2.1 ppm) used to clean the reactor. Minor bands at 1.2 ppm, ascribed to aliphatic CH₂ groups, were also found in both samples. Due to the extremely low solubility of PE in CO₂[2], these bands indicate the extraction by CO₂ of oligomers, additives, polymerisation aids or unintended added substances present in the films[3]. No aromatic signals between 6.5 and 8.0 ppm due to PET or PU monomers or oligomers were observed.

¹H NMR Comparative Spectra (DMSO d₆)

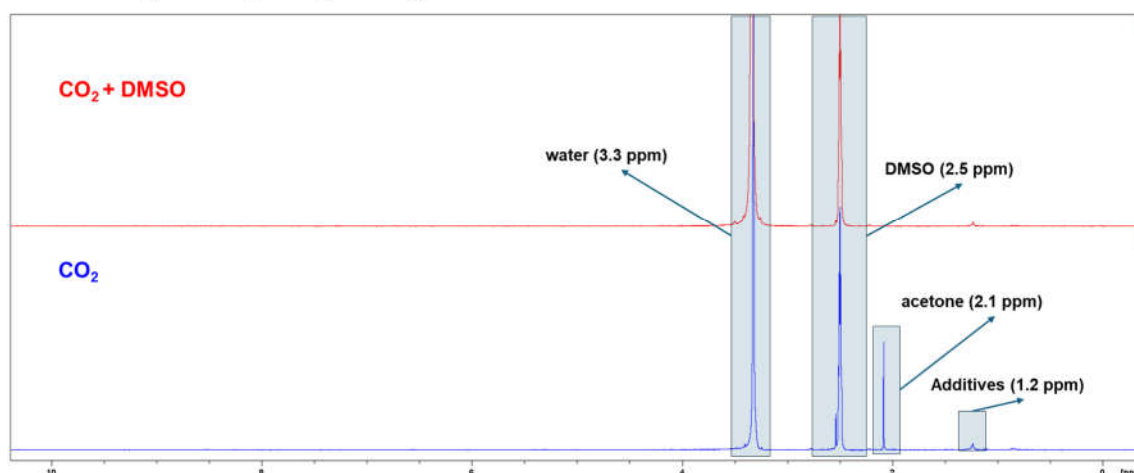


Figure S5. ¹H NMR analysis of the effluent collected after the delamination of PE/PU/PET films in CO₂ and CO₂ modified with DMSO.

References

- [1] S. Abbott, C.M. Hansen, H. Yamamoto, Hansen Solubility Parameters in Practice – Complete with software, data, and examples, 5th ed., 2015
- [2] C.F. Kirby, M.A. McHugh, Phase Behavior of Polymers in Supercritical Fluid Solvents, Chem. Reviews, 99 (1999) 565-602
- [3] B.S. Anouar, C. Guinot, J.-C. Ruiz, F. Charton, P. Dole, C. Joly, C. Yvan, Purification of post-consumer polyolefins via supercritical CO₂ extraction for the recycling in food contact applications, J. Supercrit. Fluid., 98 (2015) 25-32.